

Quantifying Cloud-Induced Shortwave Absorption: An Examination of Uncertainties and of Recent Arguments for Large Excess Absorption

D. G. IMRE, E. H. ABRAMSON, AND P. H. DAUM

Department of Applied Science, Brookhaven National Laboratory, Upton, New York

(Manuscript received 17 November 1995, in final form 22 March 1996)

ABSTRACT

The quantification of cloud-induced shortwave atmospheric absorption is a painstaking task and often the subject of contention. Several analytical methods previously used for this purpose are examined in detail applying each method to a set of collocated satellite and surface measurements of radiant fluxes taken in April of 1994 in Oklahoma. It is demonstrated that, if care is not taken, conclusions regarding cloud-induced absorption can be as much a function of the chosen analytical methods as they are of the data themselves. It is argued that the best method for determining the cloud radiative forcing ratio is from the slope of a plot of the cloud radiative forcing ratio at the surface versus the cloud radiative forcing at the top of the atmosphere and/or a normalized analog. Application of this method shows that clouds in Oklahoma, on average, induced an absorption of 4% more of the solar insolation than did clear sky. An examination is made of three recent papers that have reported cloud-induced atmospheric absorption in large excess over that which has been generally considered possible. It is shown that, once uncertainties and biases in the analytical methods are considered, the results of all three papers are consistent with conventional formulations of cloud-radiation interactions.

1. Introduction

Exactly how much shortwave atmospheric absorption is induced by clouds has long been a vexing question; it is the subject of many papers and much debate (e.g., Robinson 1959; Reynolds et al. 1975; Herman 1977; Slingo and Schrecker 1982; Stephens and Platt 1987; Foot 1988; Rawlins 1989; Nakajima et al. 1991; Chou et al. 1995; Hayasaka et al. 1995; Li et al. 1995, 1996; Wiscombe 1995). Many observational studies indicate that cloud-induced absorption may be somewhat larger than those predicted by numerical models. Various explanations for such "anomalous absorption" have been advanced including: differences between actual droplet size distributions and those used to infer absorption from the backscattering, the presence of absorbing aerosols in clouds, inaccurate modeling of the water vapor continuum, and the inability of either measurements or models to accurately account for cloud heterogeneities [for a summary see Stephens and Tsay (1990) and references therein].

Quite distinct from these previous discussions, three recent studies have appeared, which, together, argue that one particular measure of cloud absorption, the

cloud radiative forcing ratio (vide infra), is as large as 1.5 (Cess et al. 1995; Ramanathan et al. 1995; Pilewskie and Valero 1995). Such a ratio is much larger than the 0.9–1.2 commonly predicted by general circulation models (GCMs) and suggests a cloud-induced absorption so large that, if it were to exist, it would call into question our basic understanding of cloud-radiation interactions (Stephens 1996, manuscript submitted to *Science*); indeed, one of these new papers suggests the possibility of a "missing physics."

Measurements of atmospheric radiative fluxes are notoriously difficult to interpret. Given the highly variable nature of the data, and numerous past conflicting reports, it is clear that the conclusions that are derived from a given set of radiometric data are highly dependent on the details of both the experiment and the analysis. We present in this paper an analysis of collocated satellite and surface measurements of shortwave (SW) fluxes for the intensive observing period (IOP) of April 1994 at the Atmospheric Radiation Measurement (ARM) site in north-central Oklahoma. Our purpose is to use the high-quality ARM data to examine and compare various methods that have been employed in calculations of the cloud radiative forcing ratio (CRF_R), with an emphasis on the analysis of possible errors. We demonstrate that conclusions regarding anomalous absorption can be as much a function of the chosen analytical methods as they are of the data themselves. Furthermore, we show that the ARM IOP dataset clearly excludes cloud-induced absorption of the magnitude recently reported.

Corresponding author address: Dan Imre, Department of Applied Science, Brookhaven National Laboratory, Upton, NY 11973-5000.
E-mail: imre@bnlux1.bnl.gov

This paper is constructed as follows. In section 2, we present technical information (sources of data, etc.). In section 3, there is a preliminary introduction to cloud radiative forcing (CRF) and the CRF_R , followed by a comparative study of the various analytical methods used to calculate CRF_R . Each method is applied to the ARM IOP dataset. Section 4 is a case study of the effect of clouds on SW radiation at the ARM site during the IOP. Finally, in section 5, we reexamine the three recent reports of large excess absorption and demonstrate that, once reasonable uncertainties are considered, the results given in these studies do not require the invocation of a "missing physics."

2. Technical

Two sets of surface radiation data were obtained from the central facility of the southern Great Plains CART (Cloud and Radiation Test Bed) site of the ARM Program located in Oklahoma at (36.61°N, 97.49°W). Upward and downward broadband SW irradiances were obtained from the Solar and Infrared Radiation Observation Station (SIROS) for 7–27 April 1994. Direct and diffuse surface insolation was obtained from the ARM Broadband Solar Radiation Network (BSRN) from 7 through 30 April. Comparisons of SIROS and BSRN show that the average surface insolation as measured by the two instruments for this period (7–27 April 1994) differed by only 3 W m^{-2} . The data were supplied with 1-min time resolution. For comparison with satellite data, 30-min averages (15 min on each side of the satellite data) were calculated. Temporal averaging is intended to minimize errors due to unequal spatial coverage by the satellite and surface detectors. Surface albedo was calculated from the SIROS up- and down-looking radiometers and averaged 0.205 over the month.

Fluxes at the top of the atmosphere (TOA) were obtained from *GOES-7* (Geostationary Operational Environmental Satellite), every 30 min from 1330 through 2330 UTC each day during the IOP, on a $0.3^\circ \times 0.3^\circ$ grid centered on the central facility. The fluxes, derived specifically for comparison with ground data recorded during the IOP, were calculated as described in Minnis et al. (1995). The processing included a conversion of the calculated narrowband ($0.55\text{--}0.75 \mu\text{m}$) visible fluxes to broadband ($0.2\text{--}5.0 \mu\text{m}$) fluxes, based on intercomparisons of previously obtained ERBS (earth radiation budget satellite) broadband and *GOES-6* narrowband data. The actual tabulation consists of TOA albedos, which must be combined with TOA insolation to derive the fluxes. Along with the *observed* TOA albedos, the satellite product also included the expected clear-sky albedo for each pixel for the extant SZA.

We calculate the TOA insolation I_{toa} as

$$I_{\text{toa}} = 1365r^{-2} \cos(\text{SZA}) = 1365\mu',$$

where SZA is the solar zenith angle, r is the earth–sun distance in astronomical units (AU) and the insolation (W m^{-2}). The orbital correction is virtually constant throughout April in Oklahoma so that μ' is essentially proportional to the cosine of the SZA. Figure 1 shows the TOA and surface net fluxes plotted as functions of μ' .

There are two commonly used conventions for reporting atmospheric radiation data; one gives values averaged over 24 h while the second, referred to here as "day-side," gives values averaged over μ' larger than some minimum value, usually 0.2–0.3. The satellite derived data on which this paper is based include all SW fluxes with μ' greater than 0.25. Day-side average fluxes for the (April) ARM IOP data are greater by a factor of 2.3 than 24-h averages; fractional absorptions and other ratioed values are virtually identical. Throughout this paper whenever we compare our results with those of others, we attempt to follow their convention to make the comparison easier.

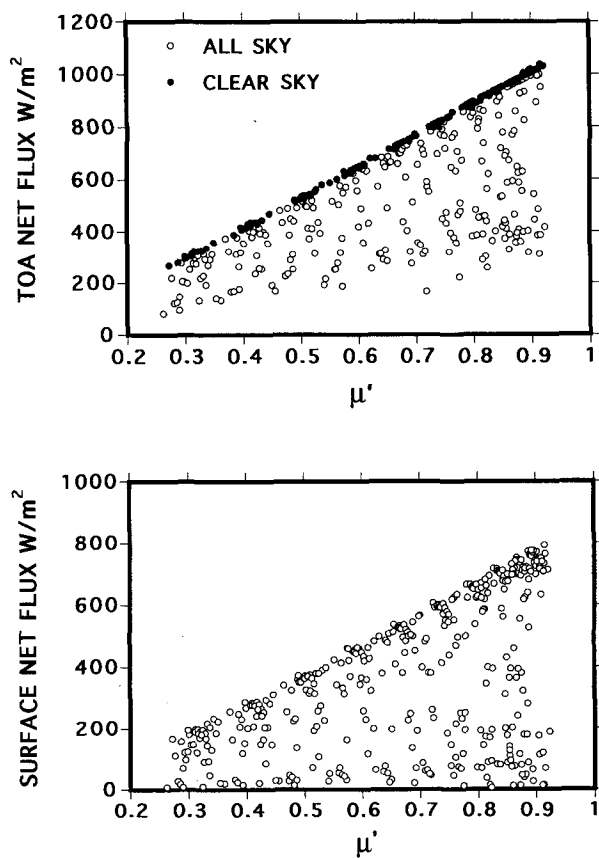


FIG. 1. Net fluxes at the top of the atmosphere (upper panel) and the surface (lower panel) for the entire (all sky) ARM IOP (SIROS) dataset. The fluxes are plotted against μ' , which closely approximates the cosine of the solar zenith angle. In the top panel the subset of points denoted by filled circles are those assigned as clear sky by the GOES product. Surface clear-sky identification is the subject of Figs. 2, 3, and 4.

In this paper we treat the satellite (GOES) data as given, although in our opinion a major question exists relating to the conversion of the satellite narrowband visible observation to the required broadband information. The validity of the use of a satellite that is completely *blind* to the near infrared to study atmospheric absorption, which is almost entirely a near infrared phenomenon is not clear. These problems are exacerbated by the relatively loose correlation between the broadband and near-infrared terrestrial surface reflectance (Li et al. 1993). We defer this question to a separate study where it will be addressed in detail.

3. Calculating the cloud radiative forcing: A comparative study of analytical methods

At least four different methods have been employed in the past for the purpose of deriving the CRF_R from collocated satellite and surface data. In this section we apply each of these methods to the current data from the Oklahoma ARM site. First, we review the definition of the CRF_R and the quantities from which it is derived to make our subsequent analysis clear.

Cloud radiative forcing is defined as the difference in net SW flux (i.e., downwelling minus upwelling) between a given atmosphere, and the *very same* atmosphere with the clouds removed. We denote these two fluxes as the all-sky flux aF and the clear-sky flux ${}^{clr}F$.

At the surface the cloud radiative forcing is

$$CRF_s = {}^aF_s - {}^{clr}F_s, \quad (1)$$

and similarly for the TOA we have

$$CRF_{toa} = {}^aF_{toa} - {}^{clr}F_{toa}. \quad (2)$$

The difference of the two forcings, $\delta_{CRF} = CRF_{toa} - CRF_s$, is the radiative power absorbed by the atmosphere due to the presence of clouds. The cloud radiative forcing ratio $\overline{CRF_R}$, is defined to be an averaged (mean) quantity (unless specifically stated otherwise):

$$\overline{CRF_R} = \overline{CRF_s} / \overline{CRF_{toa}}. \quad (3)$$

The $\overline{CRF_R}$ is defined such that it is a measure of the radiative effect of clouds on the entire atmospheric column and as such has climatic implications. $\overline{CRF_s}$ is a measure of how much less SW radiation is absorbed at the surface due to the presence of clouds while $\overline{CRF_{toa}}$ is a measure of how much of that "missing" radiation is reflected back to space. If $\overline{CRF_s} = \overline{CRF_{toa}}$, this implies that all the radiation that is "missing" at the surface has been reflected back to space, in other words the absorption by the entire atmospheric column is the same whether the clouds are present or not, the clouds are "neutral," and $\overline{CRF_R} = 1$. Similarly, $\overline{CRF_R} > 1$ implies that absorption by the entire atmospheric column for cloudy sky must be larger than that for clear sky. Note that an average CRF_R near unity in

no way implies that clouds do not absorb SW radiation. It is only a fortuitous consequence of the way clouds tend to redistribute the absorption throughout the atmospheric column, such that the net result is that the total atmospheric absorption by clouds and gases is approximately the same as the absorption by the gases alone when clouds are not present. We must also keep in mind that CRF_R 's averaged over short periods can be highly variable, depending on the specific atmospheric conditions such as cloud amount, cloud height, humidity, and SZA.

Superficially, it seems a rather straightforward task to evaluate the CRF_R given collocated, surface, and satellite radiation measurements. However, as we show below, derived values of CRF and $\overline{CRF_R}$ are extremely dependent on the *details* of the chosen analytical procedure, in particular, the exact definition of "clear sky." This sensitivity to detail is a consequence of the need to evaluate small differences between large and highly variable numbers; it is the major source of forty years of controversy.

a. The direct CRF and CRF ratio method

We first examine what we term the "direct method" in which $\overline{CRF_s}$ and $\overline{CRF_{toa}}$ are evaluated directly as the differences between clear- and all-sky net fluxes, in strict conformance with the definitions of Eqs. (1) and (2), and the $\overline{CRF_R}$ is evaluated from Eq. (3). The "all-sky" dataset comprises the data points as observed, and thus is well defined. In contrast, "the clear sky" subset of the data is a conceptual tool subject to various possible definitions. For example, in Ramanathan et al. (1995) clear sky is effectively defined for each all-sky datum as the complementary and hypothetical atmosphere, which would result from removing *only* the liquid water while leaving all else (e.g., gaseous water and aerosols) untouched. The definitions used by Cess et al. (1995 and 1993) differ significantly, in that clear-sky references were *empirically* defined as various averages of experimentally measured fluxes during times when the sky had been identified as free of clouds. To put this in perspective, we note that surface fluxes under cloud-free skies can vary by over 50 W m^{-2} due just to normal fluctuations in aerosol loading and humidity (Li et al. 1993). These variations in what might be empirically chosen as the clear-sky reference are comparable in magnitude to the difference between what is considered to be normal and anomalous atmospheric absorption. We need, therefore, a special emphasis on how the clear-sky reference is theoretically defined and, separately, determined from the data.

The all-sky data were shown in Fig. 1. To calculate the $\overline{CRF_s}$ and $\overline{CRF_{toa}}$, we need now only to choose the clear-sky references (TOA and surface) for each SZA. To generate the clear-sky reference fluxes we adopt an empirical procedure and fit a smooth function through a subset of points that are considered to represent clear

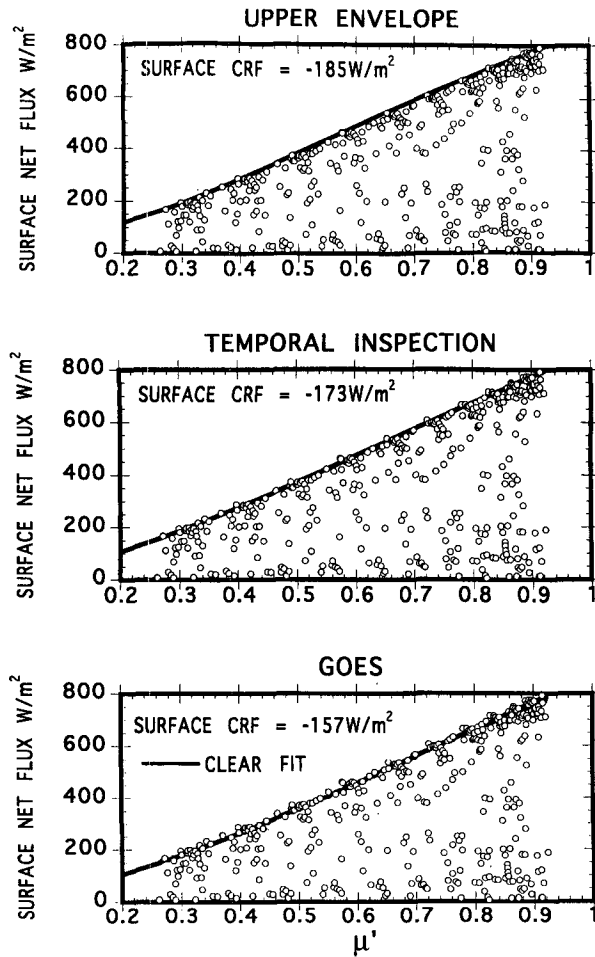


FIG. 2. Lines representing three different clear-sky references superimposed on plots of the half-hour net fluxes at the surface. Each clear-sky reference is derived from a smooth fit through the subset of clear-sky points assigned on the basis of the (a) upper-envelope, (b) temporal inspection, and (c) satellite scene identification. The different ways of assigning "clear sky" lead to significantly different values for the surface cloud radiative forcing and thus the CRF ratio (see also Table 1).

sky. In essence, the derived function represents the average, clear-sky net flux for any SZA. This function is then used as *the* clear-sky reference. The freedom in this method lies in how one chooses to assign data points as belonging to the clear-sky subset; the details of this choice can have a dramatic effect on the derived value of the $\overline{\text{CRF}}_R$. For illustrative purposes we use three different criteria for assigning points to the clear-sky subsets, and derive the corresponding value of the $\overline{\text{CRF}}_R$. The effect of these choices on $\overline{\text{CRF}}_R$ is illustrated in Fig. 2.

1) CLEAR-SKY REFERENCE BY THE UPPER-ENVELOPE METHOD

This method was used in a recent paper by Cess et al. (1995). The premise of the method is that atmo-

spheric transmission is maximized for clear sky conditions so that the maximum observed flux for each SZA is a reasonable representation of the clear sky; the clear-sky subset is composed solely of these points. This method tacitly assumes that clear sky has well-defined properties. In reality, however, clear-sky fluxes vary from day to day and season to season. For example, Fig. 3 illustrates four, clear mornings during the April ARM IOP in Oklahoma with differences in surface fluxes (Fig. 3b) of 15–20 W m^{-2} . Obviously, seasonal variations in clear-sky net fluxes are expected to be much larger.

As implied by its name, the upper-envelope method yields a clear-sky reference consistent with the clearest of clear skies, thus producing the maximum magnitude possible for $\overline{\text{CRF}}_S$ and hence a maximum $\overline{\text{CRF}}_R$ (fluxes measured at TOA exhibit much smaller fractional vari-

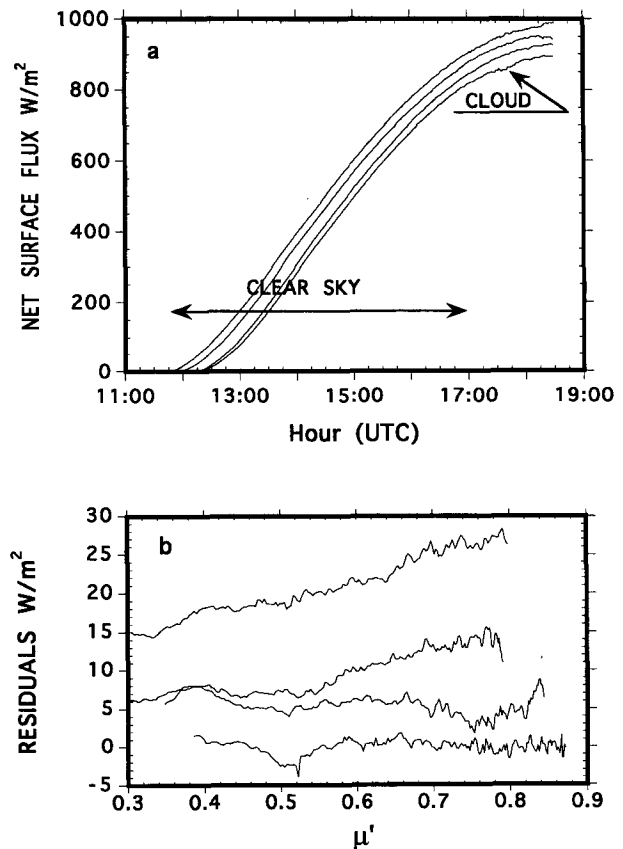


FIG. 3. Net surface fluxes for four different clear mornings (1, 3, 16, and 26 April) at the Oklahoma ARM. The top panel illustrates the smooth curves indicative of clear sky (the absence of clouds is confirmed by the satellite scene identification and also the measured ratio of diffuse to direct surface insolation). The lower panel shows the differences between the fluxes pictured in the top panel and a smooth fit through one of them. In this second graph the fluxes have been compared by μ' and the differences are due entirely to differences in the (clear) atmosphere (e.g., humidity and aerosol loading). The lower panel shows that differences in the surface clear-sky net fluxes can be as high as 20 W m^{-2} during a single month.

ations). For illustrative purposes we have chosen here only the very uppermost points at each solar zenith angle, as illustrated in the upper panel of Fig. 2. This manner of choosing a clear-sky reference yields $\overline{CRF}_s = -185 \text{ W m}^{-2}$ and for the TOA, $\overline{CRF}_{\text{toa}} = -138 \text{ W m}^{-2}$. The additional absorption due to clouds, $\delta_{\text{CRF}} = 47 \text{ W m}^{-2}$, is comparable to the variations in clear sky, which are shown in Fig. 3b. The resultant \overline{CRF}_R is 1.35, which might be considered to be consistent with a large SW cloud-enhanced absorption.

In applying this method we found it to be highly subjective in that the final clear-sky reference one obtains depends strongly on how fine a sampling in SZA one uses when binning the data. Further, as was pointed out by Cess et al. (1995), under broken cloud cover, the maximum surface fluxes can sometimes result from side reflections from clouds which will generate fluxes higher than those of clear sky. Unfortunately, there is no way to recognize these points in the usual plot of flux versus μ' .

2) CLEAR-SKY REFERENCE BY TEMPORAL INSPECTION OF SURFACE DATA

The high-temporal-resolution ARM data allow an identification of clear sky by a simple inspection of the 1-min averages of downwelling surface radiation plotted against time of day. Figure 4 illustrates two days of such data; 3 April was mostly clear with clouds in the late afternoon, whereas 13 April had a clear morning and cloudy afternoon. Clouds leave a signature, recognized as noisy traces, both in the (diminution of) total radiation and in the (increased) ratio of diffuse to direct radiation. We inspected plots of the type shown in Fig. 4 for the entire month of April and chose only sections where the data appear smooth for a few hours at a time. Clear-sky points assigned in this fashion exhibited a spread of 20 W m^{-2} about the surface clear-sky reference generated from them. This reference, labeled "temporal inspection" in Fig. 2, is on average 12 W m^{-2} lower than that from the upper-envelope method, and the mean surface forcing is thus also 12 W m^{-2} lower (in magnitude) $\overline{CRF}_s = -173 \text{ W m}^{-2}$. The corresponding TOA clear-sky reference yields a $\overline{CRF}_{\text{toa}} = -136 \text{ W m}^{-2}$, essentially the same as the -138 W m^{-2} by the upper-envelope method. The δ_{CRF} , which now results in 37 W m^{-2} and the cloud forcing ratio, $\overline{CRF}_R = 1.27$, is smaller than that calculated with the upper-envelope method.

3) CLEAR-SKY REFERENCE FROM SATELLITE SCENE IDENTIFICATION

The clear-sky reference can also be assigned on the basis of satellite scene identification. A scene is identified by the satellite as clear sky on the basis of both infrared and SW fluxes. For the satellite data that we use here the GOES-7 product includes, for every 30-

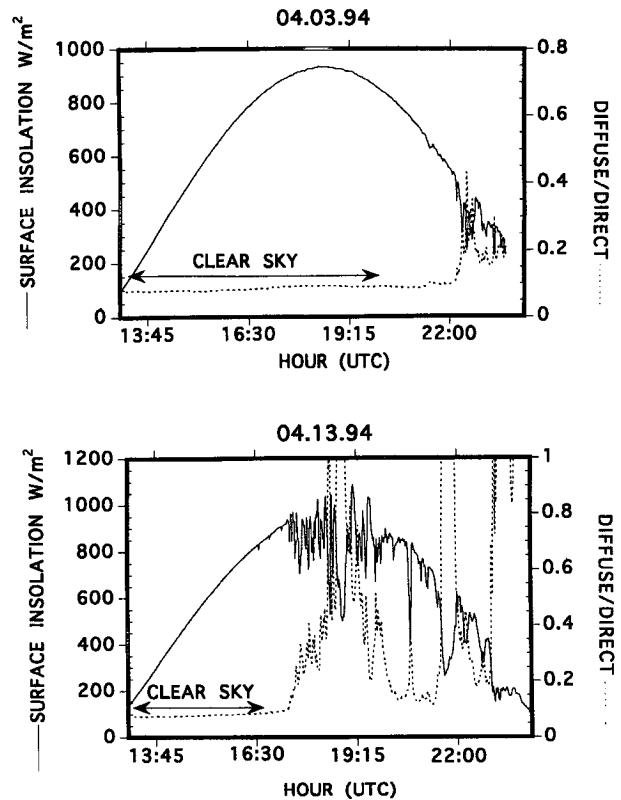


FIG. 4. Total surface insolation and the ratio of diffuse to direct insolation for two representative clear-sky days (3 and 4 April). The indicated sections have been assigned as clear sky on the basis of their smooth insolation curves and a low ratio of diffuse to direct insolation, in accord with the "temporal inspection" method.

min snapshot, an observed TOA albedo and a reference, clear-sky TOA albedo. $\overline{CRF}_{\text{toa}}$ can then be evaluated directly as

$$\overline{CRF}_{\text{toa}} = I_{\text{toa}} (\alpha_{\text{toa}} - \text{clr} \alpha_{\text{toa}}). \quad (4)$$

Here I_{toa} is the TOA insolation and α_{toa} and $\text{clr} \alpha_{\text{toa}}$ are the observed and the clear-sky reference TOA albedos. This procedure produces a clear-sky reference based strictly on what the satellite product identifies as clear sky. (These TOA clear-sky points are labeled as solid circles in Fig. 1.) We prefer this method in that the algorithms used to derive total TOA fluxes (from the narrow-angle, narrowband radiances observed by the satellite) also require identification of fractional cloud cover and, thus, are consistent with the satellite scene identification of clear sky, but perhaps not with other clear-sky choices. For the current dataset this method gives $\overline{CRF}_{\text{toa}} = -136 \text{ W m}^{-2}$, in good agreement with other methods.

Since the TOA clear-sky reference, and, thus, the $\overline{CRF}_{\text{toa}}$, are determined on the basis of the satellite scene ID, for the \overline{CRF}_R to have a physical meaning the surface clear-sky data need to be assigned in the same

TABLE 1. Surface and top of the atmosphere cloud radiative forcing calculated using three different methods for choosing the clear-sky reference. Here, δ , the difference in forcings, is the additional power calculated to have been directly absorbed by the atmosphere due to clouds; it varies by more than a factor of two with different choices of clear-sky reference. (All values are day side only.)

Clear-sky choice	$\overline{\text{CRF}}_s$ (W m^{-2})	$\overline{\text{CRF}}_{\text{toa}}$ ($\pm 14 \text{ W m}^{-2}$)	δ_{CRF} (W m^{-2})	Direct CRF_R
Upper envelope	-185	-138	47	1.2-1.5
Temporal inspection	-173	-136	37	1.1-1.4
GOES	-157	-136	21	1.0-1.3

$\overline{\text{CRF}}_s$ is the average surface cloud radiative forcing.

$\overline{\text{CRF}}_{\text{toa}}$ is the average TOA cloud radiative forcing.

CRF_R is the average cloud radiative forcing ratio.

$\delta_{\text{CRF}} = \overline{\text{CRF}}_s - \overline{\text{CRF}}_{\text{toa}}$.

way. Accordingly, we designate the surface data as clear sky for the same time periods that the satellite analysis program has designated the TOA data as clear sky. This is the procedure used by Cess et al. (1993) to identify clear sky in a study of the effect of clouds on the SW radiation budget. The bottom trace in Fig. 2 shows the clear-sky reference based on all the surface (half-hour averaged) data points corresponding to those scenes, which the satellite algorithm designated as clear. The resulting clear-sky reference is 28 W m^{-2} lower (in magnitude) than obtained from the upper-envelope method and, consequently, $\overline{\text{CRF}}_s$ is also 28 W m^{-2} lower. Combination of the surface and TOA cloud forcings now yields $\delta_{\text{CRF}} = 21 \text{ W m}^{-2}$ and $\text{CRF}_R = 1.15$.

4) SUMMARIZING THE DIRECT METHOD OF DETERMINING CRF_R

Tables 1 and 2 contain a summary of the results for this section. Table 1 gives $\overline{\text{CRF}}_{\text{toa}}$, $\overline{\text{CRF}}_s$, and the CRF_R as derived from the three different approaches outlined above. Table 2 illustrates that the two available independent datasets (BSRN and SIROS) yield identical results. Because the BSRN data included only downwelling insolation, the CRF_R was calculated from

TABLE 2. Comparison of average surface insulations measured by two different sets of instruments at the ARM site. BSRN operated for three days longer than SIROS during which days there was unusually heavy cloud cover; the (surface) CIF and $\overline{\text{CRF}}_{\text{toa}}$ are correspondingly larger for BSRN. Using GOES clear-sky references, both instruments give the same CIF ratio and, with an average surface albedo of 0.205, the same CRF_R . (All values are day side only.)

Surface detector	CIF (W m^{-2})	$\overline{\text{CRF}}_{\text{toa}}$ (W m^{-2})	Direct CIF_R	Direct CRF_R
SIROS	-197.5	-136 ± 14	1.3-1.6	1.0-1.3
BSRN	-224	-158 ± 17	1.3-1.6	1.0-1.3

CIF is the surface cloud insolation forcing.

$\overline{\text{CRF}}_{\text{toa}}$ is the average TOA cloud radiative forcing.

CIF_R is the average cloud insolation forcing ratio $\text{CIF}/\overline{\text{CRF}}_{\text{toa}}$.

CRF_R is the average cloud radiative forcing ratio.

the cloud insolation forcing (CIF) ratio,¹ and an average surface albedo of 0.205, as determined from the SIROS data, with the clear-sky references chosen by satellite scene ID. (The differences between the two surface detectors, seen in both the TOA and surface forcings, reflect the different days when the detectors were operational).

Confidence limits given for the $\overline{\text{CRF}}_R$ in Tables 1 and 2 are based solely on estimated uncertainties in the $\overline{\text{CRF}}_{\text{toa}}$. The 10.9% uncertainty we have included represents that given by Minnis et al. (1995) for the conversion of the narrowband GOES fluxes to the required broadband data. As such it represents a minimum uncertainty on $\overline{\text{CRF}}_{\text{toa}}$. Uncertainties in surface fluxes are insignificant when compared with variations due to choice of surface clear-sky reference. Use of these uncertainties in calculations of the $\overline{\text{CRF}}_R$ yields the ranges of CRF_R values given in the last column of Tables 1 and 2; these values vary from 1.0, which is consistent with the current understanding of clouds, to 1.5, which would indicate a "substantial unexplained absorption" (Cess et al. 1995).

The principal conclusion from this analysis is that the value of $\overline{\text{CRF}}_R$ derived from a given set of data depends strongly on the choice of what constitutes the clear-sky reference. The apparent simplicity of "clear sky" creates the false impression that the clear-sky reference is well defined. In fact, as we have shown, there

¹ For cases where net surface fluxes are not available (because a downward facing radiometer does not exist) the cloud insolation forcing (CIF) may be useful. This quantity is defined as the difference of all-sky and clear-sky surface insulations. In analogy with the CRF_R , an average CIF ratio (CIF_R) is defined as the quotient of CIF and $\overline{\text{CRF}}_{\text{toa}}$. The two ratios are then related by an estimated average surface albedo $\bar{\alpha}_s$ according to: $\overline{\text{CRF}}_R = (1 - \bar{\alpha}_s)\text{CIF}_R$. In principle, a comparison between model and data could be made on the basis of CIF ratios alone, if the surface albedo were accurately modeled, thereby eliminating the need for a downward facing radiometer. This approach, however, can be highly misleading if care is not taken to insure that the model properly represents the surface albedo. But, in order to ensure that model and data agree on the surface albedo it must be determined, which obviously requires a down-facing pyrometer.

is great latitude in both the formal definition of clear sky and, additionally, once defined, in its extraction from the data. This lack of attention to the clear-sky reference is carried further when, in comparisons of models with field data, any discrepancy is ascribed solely to the models' inability to reproduce the cloudy conditions; in fact, the same GCMs have consistently been shown to substantially underpredict the clear-sky atmospheric absorption (Li and Barker 1995; and Arking 1995, personal communication).

b. TOA albedo versus transmission method

Partly due to difficulties in the determination of clear-sky references, Cess et al. (1995) offer an alternative method that they suggest eliminates the need to identify clear sky.

Through use of a set of approximations, which we present in the appendix, it is possible to derive an expression that relates CRF_R to the slope, $-\beta$, of a plot of α_{toa} , the TOA albedo, versus I_s/I_{toa} , the transmission (I_s and I_{toa} are surface and TOA insolutions, respectively). Thus,

$$\beta = - \frac{d\alpha_{toa}}{d(I_s/I_{toa})}$$

If β can be reasonably approximated by a constant, that is, if α_{toa} is linearly related to transmission, then (within the other assumptions of the derivation) the CRF_R is related to the slope of that straight line according to

$$CRF_R = \frac{(1 - \bar{\alpha}_s)}{\beta}, \tag{5}$$

where $\bar{\alpha}_s$ is the average surface albedo as defined in the appendix.

Earlier in this paper we emphasized that the greatest difficulty in determining cloud forcing can actually lie in determining (and defining) the clear-sky reference. The TOA albedo slope method was presented as a method in which the identification of clear sky is not required. It is, however, difficult to accept the concept of a method that would be able to determine the difference between cloudy and clear skies without the need to identify clear skies. Closer examination of the method (see the appendix for details) reveals, however, that it contains implicit (and untested) assumptions concerning clear-sky properties. In particular, when deriving Eq. (5), one must assume that a plot of α_{toa} versus transmission for any clear-sky points (driven principally by changing SZA) will have the same slope and intercept as a similar plot for cloudy skies (driven by both the SZA and the amount of optical properties of clouds). This assumption, as shown below, is generally incorrect and can result in an incorrect value for any CRF_R calculated through Eq. (5).

Additionally, the method under discussion requires that the TOA albedo be linearly related to the trans-

mission. Such a relation has never been demonstrated to be supported by data. In fact, all the datasets that we have examined thus far exhibit curvature similar to that found in the ARM IOP dataset (vide infra).

The most common justification for using the linear approximation is that GCMs give a linear relation, and it is thus reasonable to assume linearity as a basis for comparison. However, the fact that the data do not support this prediction indicates only that *something* within the models is wrong. But since the observed nonlinearity indicates that the plot's "slope" cannot be equated with the CRF_R , differences in the slopes do not necessarily imply that the CRF_R 's themselves are different.

1) APPLICATION TO THE ARM SITE DATA

Despite the our misgivings we nevertheless apply this method to the ARM IOP dataset. In Fig. 5, TOA albedos, derived from the 30-min satellite snapshots, are plotted against 30-min averages of surface transmission as obtained from the BSRN dataset. For the purpose of illustration, some of the clear-sky points are depicted by different symbols. Also shown is a straight-line fit to the data. The slope, $-\beta = -0.72$, is deter-

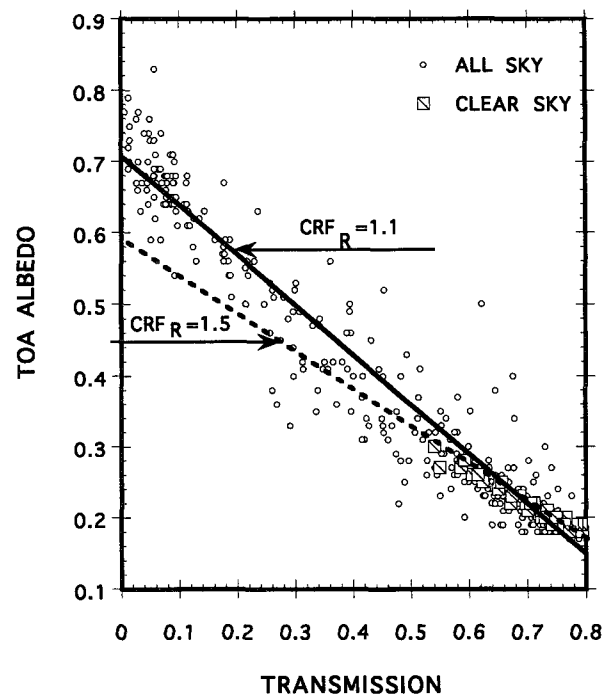


FIG. 5. Plot of top of the atmosphere albedo against transmission for the entire (BSRN) dataset. Representative clear-sky points are denoted as squares. The solid line is a result of a linear, least squares fit, for the entire dataset minimizing deviations equally in TOA albedo and transmission. The resultant straight line ($R = 0.97$) has a slope of -0.72 and an intercept of 0.705 . A separate fit through the clear-sky points only (not shown) gives a slope of -0.46 . For comparison, the dashed line corresponds to a CRF ratio of 1.5 .

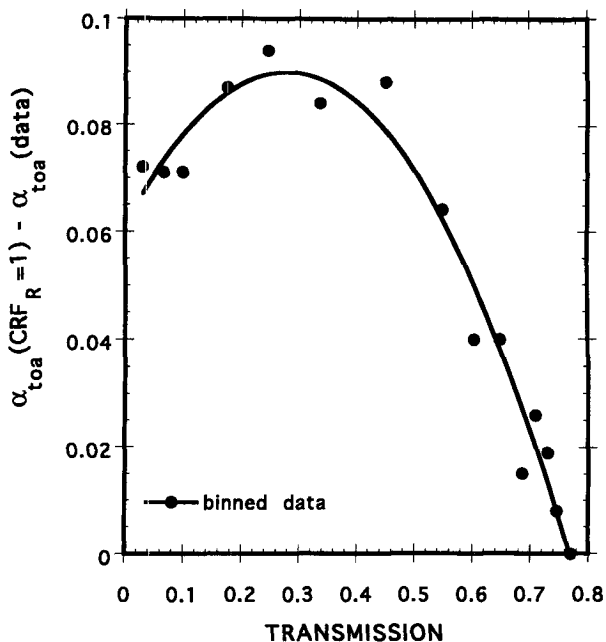


FIG. 6. Plot of the difference between the data in Fig. 5 and a straight line representing the canonical value of $\overline{CRF}_R = 1$. The resultant differences were binned by transmission to remove scatter. It is precisely this deviation from $\overline{CRF}_R = 1$ that, in the method under discussion, is quantified through a straight-line fit.

mined as the geometric mean of the two slopes obtained by regressing TOA albedo against transmission and vice versa; the correlation coefficient is $R = 0.97$. The \overline{CRF}_R calculated from Eq. (5) using the average surface albedo (0.205) measured during the April IOP is 1.1. This \overline{CRF}_R is comparable to that computed with the direct method, with the GOES clear-sky reference, although this agreement may be fortuitous.

Our misgivings as to the validity of this method stem partially from doubt as to whether a straight-line fit can be used to derive the \overline{CRF}_R . A simple inspection of Fig. 5 shows that a straight line does reproduce the general trend of the data. However, the question at hand does not concern general trends but rather small deviations in slope, which might be caused by differences in the CRF ratio from the "neutral" value of 1. Better intuition can be obtained from a plot of the deviation of the data from a line representing a \overline{CRF}_R of 1. Such a plot is shown in Fig. 6. The plot is obviously not linear and yet it is precisely this nonlinear deviation that we are attempting to quantify by means of a straight-line fit.

We have also noted that the validity of Eq. (5) depends on the assumption that the clear-sky data fall on the same line as the cloudy-sky data. A test of this assumption for the ARM IOP data reveals that the line obtained through a least squares fit of the clear-sky data has a slope of -0.46 ($R = 0.88$), significantly lower than that for cloudy-sky, thus invalidating this assumption.

2) SUMMARIZING THE TOA ALBEDO VERSUS TRANSMISSION SLOPE METHOD

Analysis of the ARM site IOP data using a plot of TOA albedo versus transmission results in an average CRF ratio of 1.1; an estimate of uncertainty based *only* on the uncertainty in the regression coefficient gives \overline{CRF}_R between 1.07 and 1.13. However, the errors in this method are not accurately represented by the statistics from the regression analysis but rather stem from the erroneous assumptions inherent to the method. These assumptions make this an unreliable technique subject to unquantifiable uncertainties.

c. TOA flux to surface flux method

Here, we examine a second method that does not require an explicit identification of clear-sky reference to obtain a \overline{CRF}_R . Instead, the \overline{CRF}_R is extracted from an analysis of the relationship between the all-sky TOA net flux and the corresponding net flux at the surface.

Cess et al. (1993) point out that if it is assumed that the net surface and TOA fluxes are linearly related, then the slope of that line contains information about atmospheric absorption. They also point out that there are two major drivers in such a plot, the SZA and cloud-

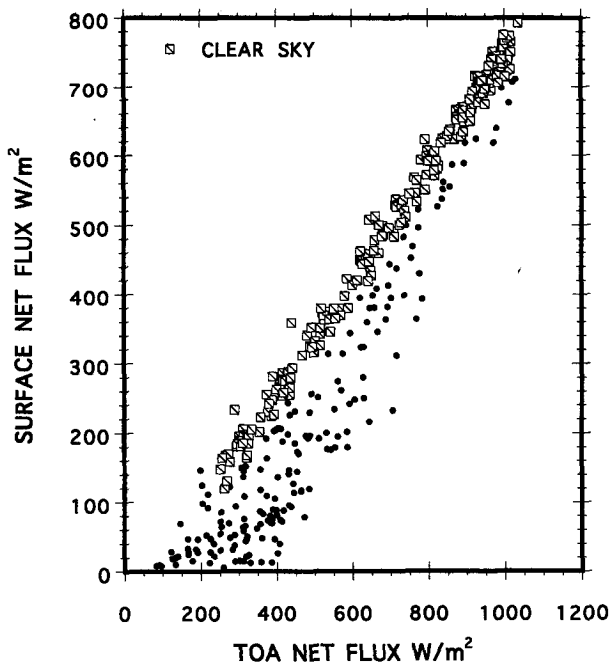


FIG. 7. Illustration of the problems associated with the use of a plot of surface flux against TOA flux for the extraction of cloud radiative effects. The entire SIROS dataset is shown; points identified by the GOES product as corresponding to clear sky are denoted by squares. The fact that the clear-sky points extend over this entire plot explains why the effect on the slope of a changing SZA is comparable to that of clouds. A partial solution to this problem is presented in Fig. 8.

ness. This is clearly illustrated in Fig. 7 where a flux to flux plot of the ARM site data is presented. The clear-sky points (designated by squares) span almost the full range of the plot due mostly to variations in SZA. The other points, of course, are affected both by cloudiness and SZA.

In an attempt to address this problem, Nemesure et al. (1994) presented an analysis of data from the Boulder Atmospheric Observatory (BAO) in combination with satellite data from the Earth Radiation Budget Experiment (ERBE). The investigators attempted to separate the effects of SZA from those of cloudiness by using a two variable regression. They assumed that surface net flux can be expressed as a function of both the TOA flux and the SZA according to

$$F_s = C + \gamma F_{\text{toa}} + \lambda \cos(\text{SZA}),$$

in which C is a constant, γ is independent of SZA, and λ is independent of cloud cover. Within the context of their assumptions $\overline{\text{CRF}}_R$ is

$$\overline{\text{CRF}}_R = \left(\frac{\partial F_s}{\partial F_{\text{toa}}} \right)_{\text{SZA}} = \gamma. \quad (6)$$

When the authors applied this method to the BAO/ERBE data they found a CRF ratio of 0.98 ± 0.05 . As a result of this analysis they concluded that “the snow-free Boulder data indicate, in the context of a seven-month mean, that the SW radiative cloud impact is neutral.” In the context of the current claims of large excess absorptions this is a particularly interesting conclusion to which we will return in section 5.

1) APPLICATION TO THE ARM SITE DATA

An inspection of Fig. 7 suggests to us that, because of the strong dependence of the fluxes on SZA, a two variable regression to an arbitrary functional form would be unlikely to isolate the true cloud forcing. If, however, a subset of the data with fixed SZA were taken, and plotted in the same manner, the slope of that line would be the $\overline{\text{CRF}}_R$ for that SZA (Cess et al. 1993). We illustrate such a procedure in Fig. 8 where a plot of TOA flux versus surface flux is shown, limited to points with $\mu' > 0.75$, for the current dataset. A straight-line fit through the data gives a $\overline{\text{CRF}}_R$ of 1.12 ± 0.1 (based on the geometric mean of slopes, for $R = 0.97$). For comparison, a line corresponding to a $\overline{\text{CRF}}_R$ of 1.5 is also shown. The slope of 1.12 agrees with the output of the European Centre for Medium-Range Weather Forecasts Global Circulation Model (ECMWF GCM) as analyzed by exactly same approach (Cess et al. 1993). In that paper, surface and TOA fluxes as predicted by the model were plotted for four different times of day and CRF ratios were derived; the calculated midday CRF ratios ranged from 1.1 to 1.2.

We attempted to analyze the rest of the data in the same fashion, in order to compute an average $\overline{\text{CRF}}_R$ for

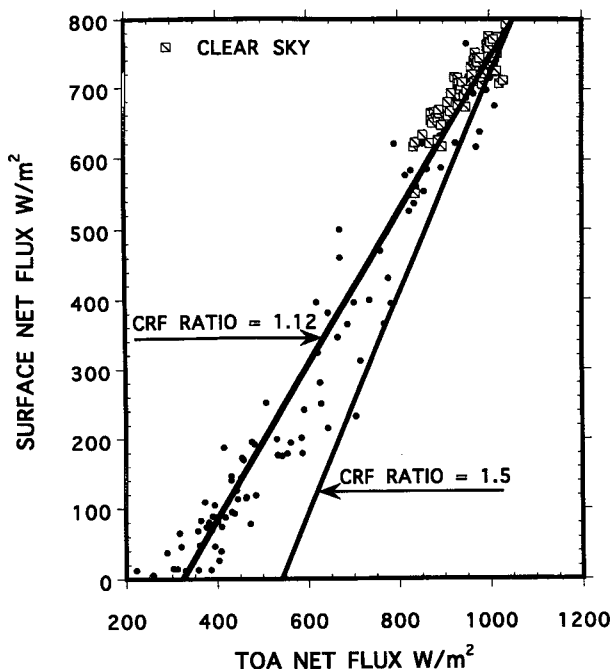


FIG. 8. As in Fig. 7, the surface flux is plotted against TOA flux, but the plot is limited to those data within a narrow range of SZA ($0.75 < \mu' < 0.92$). Clear-sky points are again identified by squares. Note that in this plot the fluxes vary mostly due to the presence of clouds and not the changing SZA. A straight-line fit through these data has a slope of 1.1, which may be equated with the CRF ratio (for this limited range of SZA). For comparison, we also show a line whose slope corresponds to a CRF ratio of 1.5.

the entire day and month, but were not able to do so; the sparsity and large scatter in the data for other values of the SZA do not allow for meaningful results.

2) SUMMARIZING THE FLUX TO FLUX METHOD

Clearly, the major drawback of this method is that fluxes are strongly dependent on two variables, which makes it difficult to separate effects due to each of these variables without dividing the data into narrow ranges of SZA, a requirement that limits the method to large datasets. In addition, the resultant $\overline{\text{CRF}}_R$ (for the different SZA's) would then need to be converted to a representative average $\overline{\text{CRF}}_R$ if the interest were in the climatic effect of clouds.

d. TOA CRF versus surface CRF method

In this section, a fourth method for deriving $\overline{\text{CRF}}_R$, as employed by Li and Moreau (1996), is examined. This method incorporates features of the direct method, in that it requires a point-by-point calculation of $\overline{\text{CRF}}_s$ and $\overline{\text{CRF}}_{\text{toa}}$ and, thus, an explicit choice of clear-sky reference, but unlike the direct method, the $\overline{\text{CRF}}_R$ is reasonably insensitive to errors in how this reference is chosen. As with the two previous methods it relies on

an assumption of linearity. Here, a linear relationship between the CRF_s and the CRF_{toa} is assumed, an assumption which we demonstrate is reasonably supported by the ARM data. One reason a plot of CRF_s versus CRF_{toa} is particularly useful is that every point has already been referenced to a clear-sky point of the same SZA, greatly reducing the influence of SZA as a driver; aside from statistical noise all the clear-sky points will now be near the origin.

We assume that, point by point, the CRF_s and CRF_{toa} are related by

$$CRF_s = CRF_R \times CRF_{toa}.$$

This equation includes the logically necessary constraint that when cloud forcing at the TOA is zero (i.e., for clear sky) cloud forcing is also zero at the surface.

As we pointed out previously, the most ambiguous task in calculating CRF_R is in choosing the surface clear-sky reference. Here we show that calculation of CRF_R using this method is relatively independent of how the clear-sky reference is chosen. Assume for the moment that the clear-sky reference is shifted by a random amount Δ from the hypothetical clear-sky reference, then each calculated CRF'_s on the basis of this erroneous clear-sky reference is shifted from the "true" CRF_s by Δ ; that is,

$$CRF_s = CRF'_s - \Delta,$$

and

$$CRF'_s = \Delta + CRF_R \times CRF_{toa}. \quad (7)$$

Note that, despite the fact that the surface cloud forcings are "wrong," CRF_R is still given by the slope of a straight-line fit, and the error due to choice of the clear-sky reference will be expressed as the intercept of value Δ , the average error. In essence, this approach assures that choice of clear-sky reference does not determine CRF_R , moreover, the intercept is a measure of how far off the chosen clear-sky reference was from its hypothetical value, which requires that the intercept of this plot be zero.

In this method, the clear-sky reference for the surface data is implicitly fixed by 1) the TOA clear-sky reference in conjunction with the requirement that, *on average*, if the TOA forcing is zero then so is the surface forcing, 2) the assumption that a straight-line fit is appropriate to the data in this representation, and 3) the assumption that the Δ are random with respect to CRF_s . These assumptions will be shown to be consistent with the ARM data to which we apply them below.

1) APPLICATION TO THE ARM SITE DATA

Figure 9 shows a plot of CRF'_s versus CRF_{toa} for the ARM data along with a straight-line fit (solid line). In this plot both clear-sky references were based on the

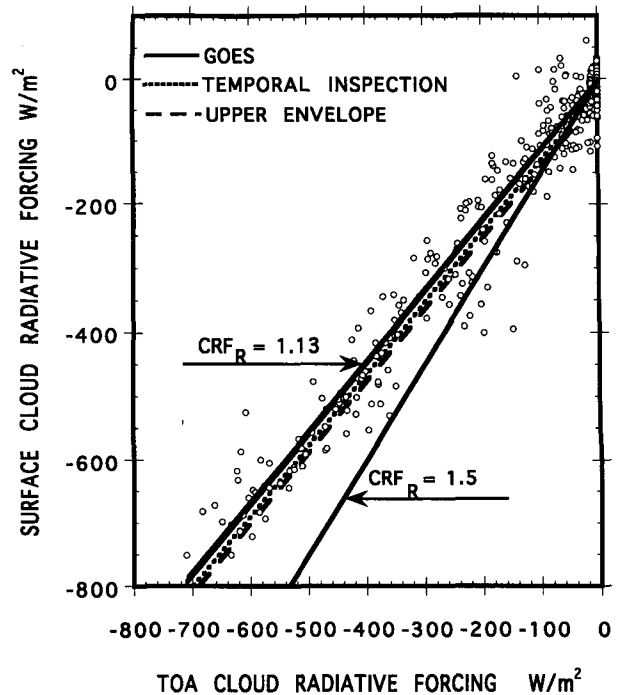


FIG. 9. Plot of surface cloud radiative forcing against TOA cloud radiative forcing as calculated on the basis of the (surface and TOA) clear-sky references, which were identified by the GOES product. In such a plot, all clear-sky points cluster around the origin, even though the entire dataset is included. A solid straight line with a slope of 1.13 represents the fit through these points. The slope of this line is the CRF_R [Eq. (7)]. The dotted and dashed lines represent fits through the data as they are calculated with the temporal-inspection and upper-envelope clear-sky references, respectively. For comparison, we again show a line whose slope corresponds to a CRF ratio of 1.5.

GOES product. The other lines in the figure depict fits as calculated from the two other methods for assigning surface clear-sky that were discussed in section 3; the three different ways of specifying the surface clear-sky reference manifest themselves only as differences in the intercepts of the plots. In agreement with our assumption, the slopes are independent of which clear-sky reference was used.

In Fig. 10, we plot the residuals between the data and the linear fit. In sharp contrast to a plot of TOA albedo versus transmission (Fig. 6), no obvious non-linear pattern is observed, indicating that CRF_R may be reasonably approximated by the slope of the linear fit. The errors introduced by this assumption are small compared with other inherent uncertainties.

We find from the slopes in Fig. 9 a CRF_R of 1.1 ($R = 0.97$). For comparison, we have also included in Fig. 9 a line corresponding to a CRF_R of 1.5. The data clearly do not support such a high value. Application of this method to the BSRN data together with an average surface albedo of 0.205 gives the same results.

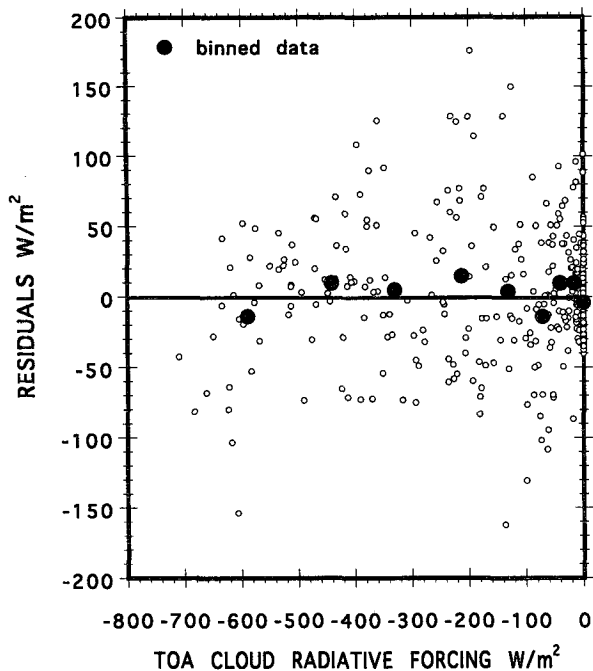


FIG. 10. Illustration of a direct test of the appropriateness of a straight line fit of the surface versus TOA forcing. The difference between the data in Fig. 9 and the straight-line fit is plotted both for the individual points and the binned product. There is no obvious curvature to the residuals, which supports the assumption that the averaged data are adequately represented by a straight line and that it is reasonable to equate the slope of such a line with the CRF_R .

2) THE ANALOGOUS PLOT, WITH FORCINGS NORMALIZED TO THE TOA INSOLATION

A slight variant of the method uses the slope of a straight-line fit to a plot of CRF_s/I_{toa} versus CRF_{toa}/I_{toa} , the *normalized* surface and TOA forcings. This is not, as it might first appear, a mere repetition of the CRF_s versus CRF_{toa} plot, rescaled by I_{toa} . The normalization serves to completely rearrange the data, therefore serving as a rigorous cross check on the CRF_s versus CRF_{toa} method. The requirement that the two methods produce the same result ensures that we do not overlook any possible systematic variation of the trial clear-sky reference with SZA. In this plot the intercept is given by Δ/I_{toa} . Analysis of the ARM site data, shown in Fig. 11, gave slopes of 1.1 ($R = 0.97$) for each plot, virtually identical to that obtained from the CRF_s versus CRF_{toa} plot. As was the case with the CRF_s versus CRF_{toa} method the three different surface clear-sky choices gave the same slope, but different intercepts.

3) SUMMARIZING THE CRF_s VERSUS CRF_{toa} METHOD

We conclude that a plot of CRF_s versus CRF_{toa} and its normalized analog CRF_s/I_{toa} versus CRF_{toa}/I_{toa} , provide an analytical method that avoids many of the prob-

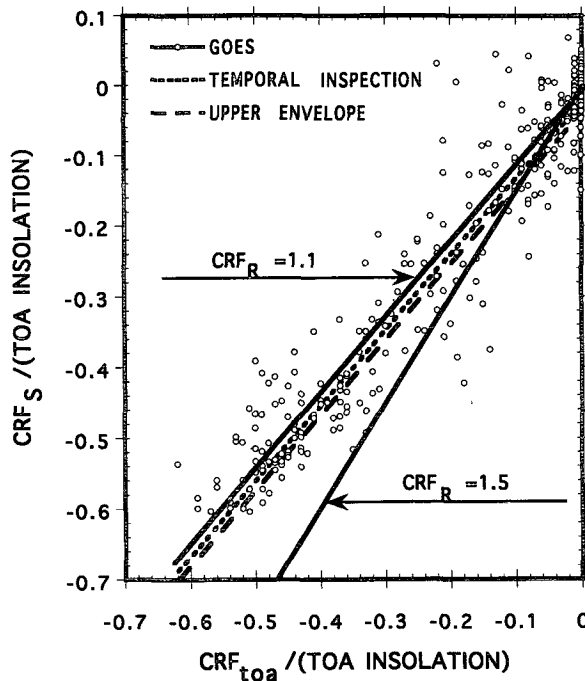


FIG. 11. For the same data used in Fig. 9, a plot of surface and TOA radiative forcings, *normalized by the TOA insolation*, as calculated on the basis of (surface and TOA) clear-sky references as identified by the GOES product. The solid straight line with a slope of 1.1 (which can be equated to the CRF_R) represents the fit through these points. The dotted and dashed lines represent fits through the data calculated using the temporal-inspection and upper-envelope clear-sky references, respectively. For comparison, a line whose slope corresponds to a CRF_R of 1.5 is also shown.

lems in the other three methods; the resultant $\overline{CRF_R}$ is reasonably independent of surface clear-sky choice, the assumption of linearity is supported by the data, and difficulties stemming from large variations in SZA are minimal. We conclude based on these methods that the data indicate a $\overline{CRF_R}$ of 1.1 (for a TOA clear-sky reference consistent with the GOES scene ID), and we have now only to estimate the associated uncertainty.

If all was perfect, the surface clear-sky reference based on GOES would have given an intercept consistent with the TOA reference from GOES—that is, an intercept identically equal to zero. Different methods

TABLE 3. Average power and percentage of the average TOA insolation that would be absorbed at the ARM site during (from left to right) a day with continually clear skies, a day with skies of average cloudiness, and a day during which the average cloudiness is altered by the removal of any clear skies.

	Clear-sky	All-sky	Cloudy-sky
Absorbed ($W\ m^{-2}$, day side only)	206 ± 5	225 ± 15	238 ± 15
Percent absorption	22.4 ± 0.5	24.6 ± 1.5	26.2 ± 1.5

of fitting cause the intercept to vary from -6 to 0 W m^{-2} . We take this to be a fair measure of the possible error in the surface forcing [see Eq. (7)] as calculated by the direct method with a GOES reference (-157 W m^{-2}). This estimate is also comparable to the average difference in surface forcings (2.5 W m^{-2}) calculated from SIROS and BSRN. We thus estimate the average $\overline{\text{CRF}_s}$ to have an uncertainty of $\pm 2\%$. $\overline{\text{CRF}_{\text{toa}}}$, as stated above, is still associated with a minimum uncertainty of $\pm 10.9\%$, due only to the necessary narrow- to broadband conversion. Propagating these errors yields a CRF_R of 1.1 ± 0.14 . Because the narrow- to broadband conversion represents only one source of uncertainty in the $\overline{\text{CRF}_{\text{toa}}}$, we cannot on this basis alone conclude that these data exclude a $\overline{\text{CRF}_R}$ of 1.5. We can, however, say that for the CRF_R to be 1.5, the overall error in $\overline{\text{CRF}_{\text{toa}}}$ must be larger than 30 W m^{-2} , which in our opinion would be unreasonable. If, on the other hand, the error is of that magnitude, this implies that all GOES based studies must be considered inconclusive.

4. Beyond the CRF ratio: A detailed examination of the Oklahoma data

a. Clear-sky, all-sky, and cloudy-sky average SW atmospheric absorption at the ARM site

We have been addressing the question of whether clouds enhance SW atmospheric absorption. Given the available data there is no compelling reason to resort to constructs such as the CRF_R . The data that are required to calculate $\overline{\text{CRF}_R}$ are also sufficient for calculating the absorption directly as

$$\overline{\%Abs} = 100 \frac{\overline{F_{\text{toa}} - F_s}}{\overline{I_{\text{toa}}}} \quad (8)$$

Here, $\overline{\%Abs}$ is the average percentage SW atmospheric absorption, $\overline{F_{\text{toa}} - F_s}$, is the average net flux difference, and $\overline{I_{\text{toa}}}$ is the average TOA insolation.

Application of Eq. (8) to the ARM site data yields the results summarized in Table 3 for the (GOES) clear-sky subset, all-sky, and the complement to the clear-sky subset, which is denoted as ‘‘cloudy sky.’’

We conclude that SW all-sky atmospheric absorption at the ARM site during April, was $2.3\% \pm 2\%$, higher than that for clear sky, or that on average the presence of clouds has resulted in $20 \pm 20 \text{ W m}^{-2}$ (day-side) excess absorption over that of a perpetually clear sky. This number should be compared with a predicted (Cess et al. 1995) excess absorption of 68 W m^{-2} (day-side), based on a hypothesized $\overline{\text{CRF}_R}$ of 1.5 and the observed $\overline{\text{CRF}_{\text{toa}}}$ at the ARM site. Such a large excess absorption is clearly outside the range of our observations.

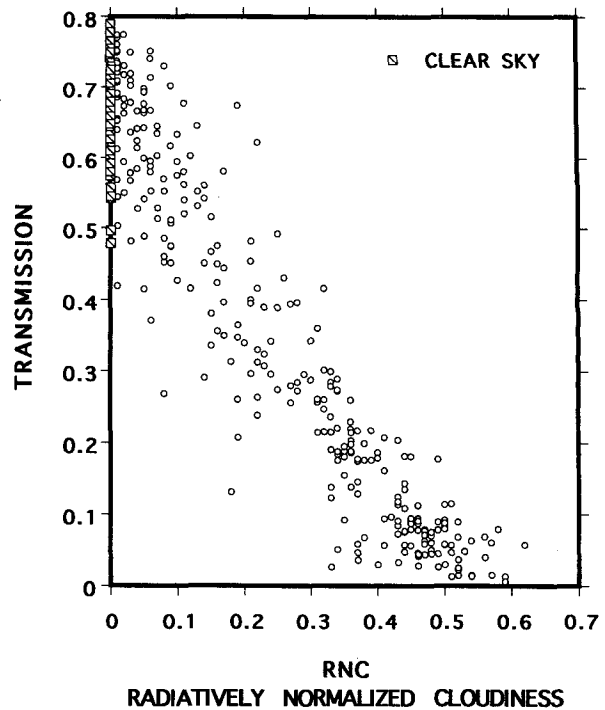


FIG. 12. Plot of transmission versus ‘‘radiatively normalized cloudiness’’ for the April IOP ARM data. Note that all clear-sky points have a cloudiness of zero, while their transmissions range from about 0.5 to 0.8 due mainly to variations in the SZA thereby illustrating that use of ‘‘radiatively normalized cloudiness’’ to represent cloud amount removes the effect of SZA.

b. Radiatively normalized cloudiness (RNC), absorption, and the CRF ratio

One of the more intriguing conclusions presented in Cess et al. (1995) is that not only does $\overline{\text{CRF}_R}$ have a value of 1.5, but that it is independent of location, cloud type, cloud amount, and latitude. Below, we use the April ARM IOP data to investigate the effects of both radiative normalized cloudiness (RNC), defined below, and SZA on atmospheric absorption (and $\overline{\text{CRF}_R}$).

1) RADIATIVELY NORMALIZED CLOUDINESS (RNC) AS A QUANTITY

We find it useful to define a new, unitless quantity, ‘‘radiatively normalized cloudiness (RNC)’’ as

$$\text{RNC} = \frac{-\text{CRF}_{\text{toa}}}{I_{\text{toa}}} = -(\text{clr}\alpha_{\text{toa}} - \text{a}\alpha_{\text{toa}}). \quad (9)$$

Here, $\text{clr}\alpha_{\text{toa}} - \text{a}\alpha_{\text{toa}}$ is the difference between clear and all-sky TOA albedo. RNC is the normalized (to TOA insolation) cloud radiative forcing at the TOA. Other units that have been used to represent cloud amounts such as TOA albedo, transmission, or CRF_{toa} suffer from the fact that they are strong functions not only of cloud amount but of SZA as well. RNC, on the other

hand removes the SZA effect almost entirely. To calibrate ourselves against a more familiar quantity, Fig. 12 shows a plot of transmission versus RNC. An RNC of 0.6 corresponds to very thick Oklahoma clouds—that is, transmission nearly zero—while a RNC of 0 corresponds to the clear-sky reference. Note that the clear-sky points range on the transmission axis from 0.8 to 0.55, due mostly to variations in SZA.

A quantitative connection between $\overline{CRF_R}$, atmospheric absorption, and RNC is given by

$$\overline{\%Abs} = \overline{\%^{clr}Abs} + \frac{\overline{CRF_{toa}}}{\overline{I_{toa}}} (1 - \overline{CRF_R}) 100. \quad (10)$$

According to Eq. (10) the all-sky average SW absorption, $\overline{\%Abs}$, can be thought of as the average clear-sky absorption, $\overline{\%^{clr}Abs}$, plus the cloud-induced absorption as given by the second term in the equation. The cloud-induced absorption is zero for a $\overline{CRF_R}$ of 1, as expected, and it is proportional to both $(1 - \overline{CRF_R})$ and $(\overline{CRF_{toa}}/\overline{I_{toa}})$, the latter of which we have defined as the average RNC. Since both the average RNC and the average clear-sky absorption vary from one location to the next, and from season to season, so will the exact relation between absorption and $\overline{CRF_R}$.

2) RADIATIVELY NORMALIZED CLOUDINESS AS IT AFFECTS ABSORPTION AND THE CRF RATIO

To examine the effect of RNC on atmospheric absorption during April at the ARM site, we calculate the absorption for each of the 30-min averaged data points as shown in Fig. 13 (open symbols). Clear-sky atmospheric absorption (RNC = 0) ranges broadly from about 18% to 30% due mainly to variations in the SZA (see Fig. 15). The absorption for the cloudy atmosphere (RNC > 0) shows a great deal of scatter, especially for the thinner clouds ($0 < \text{RNC} < 0.3$), which makes it difficult to detect a pattern. In the same figure, filled circles are used to depict the data as binned by RNC. In the binned data we see a trend of increased absorption up to about 30% for an RNC of 0.3 and then a decrease back to 23% for the thickest clouds. This variation of absorption with cloudiness is not unexpected given that the satellite data indicate that generally, the thickest clouds correspond to conditions with high cloud tops. As shown by Li and Moreau, (1996), the effect of clouds on atmospheric absorption is tightly correlated with cloud height with low clouds tending to increase atmospheric absorption, and high clouds reducing absorption by reflecting the light back to space before it has a chance to be absorbed.

Figure 14 is a plot of the individual CRF_R as a function of RNC. Again, the scatter in the region of thin clouds is rather large; this large scatter is most likely a consequence of measurement error, CRF_R being a quotient of small differences of large numbers, but as

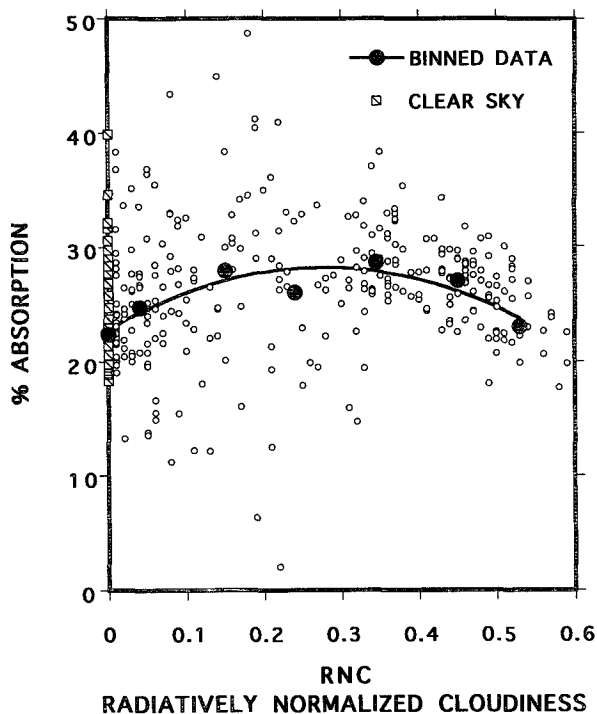


FIG. 13. Percent absorption versus radiatively normalized cloudiness. Clear-sky points are denoted by squares, cloudy-sky points by open circles. The filled data points represent the average absorption calculated for data binned by radiatively normalized cloudiness (bin width 0.1 unit). The binned data exhibits a rough trend of absorption increasing, and then decreasing, with radiative cloudiness.

clouds get thicker and the cloud forcings increase, the CRF ratio approaches 1. This plot is virtually identical to that presented in Li et al. (1996) where monthly averaged data were shown.

c. SZA, absorption, and the CRF ratio

In this section we ask whether the data support the hypothesis that the cloud forcing ratio is independent of SZA.

The upper panel of Fig. 15 shows the clear-sky absorption as a function of μ' , while the lower panel shows cloudy points *only*. As expected, the clear-sky absorption varies strongly with the SZA, but the average absorption in cloudy skies is virtually constant; the high-scattering cross sections of the cloudy skies make the photons forget their original direction. The strong dependence of clear-sky absorption on SZA, coupled with the relative independence of cloudy-sky absorption, implies that CRF_R must be a function of SZA. This dependence is illustrated in Fig. 16. CRF_R is largest ($CRF_R \sim 1.2$) when the sun is near zenith and it decreases to 0.8 as the sun moves lower in the sky. That is, as the sun approaches the horizon, the effect of clouds tends to reverse, from increasing atmospheric

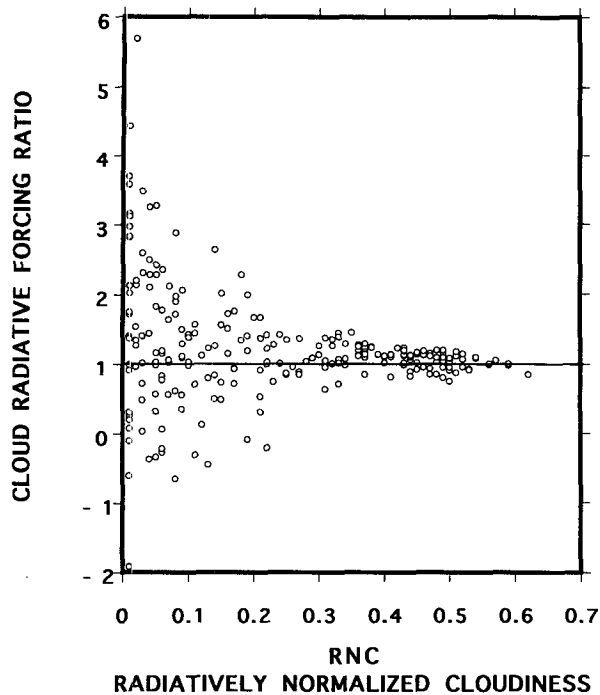


FIG. 14. Plot of \overline{CRF}_R as a function of radiatively normalized cloudiness. This plot is analogous to a similar plot presented in Li and Moreau (1996) of \overline{CRF}_R versus $\overline{CRF}_{\text{los}}$ for worldwide monthly averaged data. Both plots show very large scatter for thin clouds but as the cloudiness increases the scatter diminishes and the ratio tends to a value of approximately 1.0.

absorption to decreasing it. These results are in excellent agreement with those of the model presented in Li et al. (1996). The results also indicate that one should expect the yearly \overline{CRF}_R to increase with decreasing latitude (as was also found by Li et al. 1995, 1996).

The observed behavior can be rationalized if one considers that the one important mechanism by which clouds alter atmospheric absorption is by changing the path of the light. When the sun is at zenith the light takes the shortest path through clear sky, and scattering due to clouds can easily increase that path, thereby increasing absorption. When the sun is near the horizon, the clear-sky atmospheric pathlength is already very long, and introduction of a highly scattering medium such as clouds can result in a decrease in pathlength and thus a decrease in absorption.

5. Reexamination of recent claims of anomalous absorption

Several of the methods we have examined were recently used to infer a cloud-induced atmospheric absorption in large excess over what has been generally considered possible. Our findings concerning the uncertainties in these methods, combined with our conclusions based upon an analysis of the ARM IOP data,

suggest that claims of excessive absorption should be viewed with some caution. We have demonstrated that in any attempt to quantify cloud-induced absorption unusual care must be taken in the analysis of data, with particular attention to the realistic estimation of errors. We have also shown reason to believe that at least two of the methods used to infer excessive absorption can be subject to substantial biases. Moreover, the analysis of ERBE and Global Energy Balance Archive data presented in Li et al. (1995, 1996), a recent in situ experiment (Hayasaka et al. 1995), a theoretical analysis of the consequences of a \overline{CRF}_R as large as 1.5 (Chou et al. 1995), a study of cloud forcing based on the International Satellite Cloud Climatology Project (Laszlo and Pinker 1993), and an analysis of the Cess et al. (1995) study by Stephens (1996), all indicate that the \overline{CRF}_R is not significantly higher than predicted by conventional models. It seems reasonable, therefore, to re-

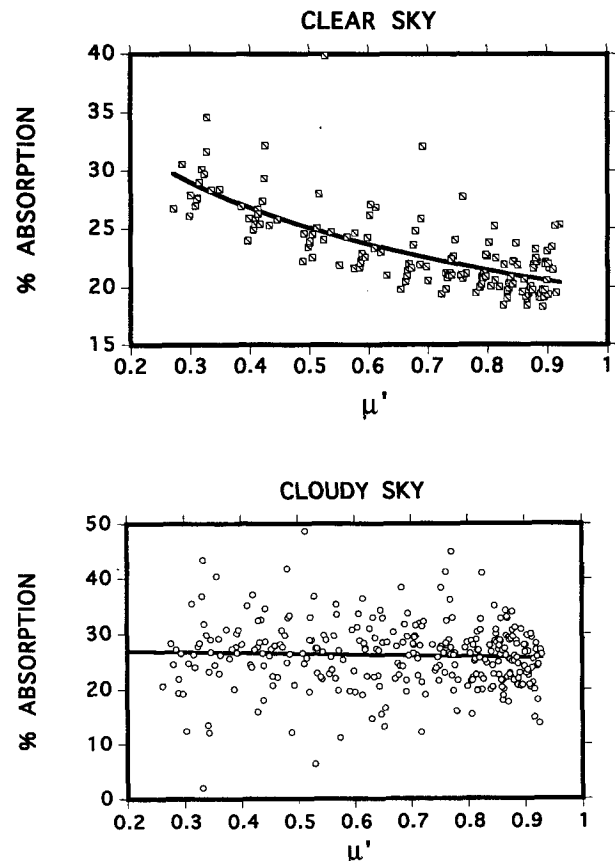


FIG. 15. Percent absorption versus μ' for individual points belonging to the clear-sky (upper panel) and cloudy-sky (lower panel) subsets to illustrate the effect of SZA on SW atmospheric absorption. For clear skies, as the sunlight travels through more of the atmosphere (decreasing μ'), the absorption, on average, increases from about 18% to 30% (upper panel). Absorption in cloudy skies (lower panel) is not appreciably affected by SZA. Considered together, these two plots suggest that \overline{CRF}_R must vary with SZA and, by extension, latitude (see Fig. 16).

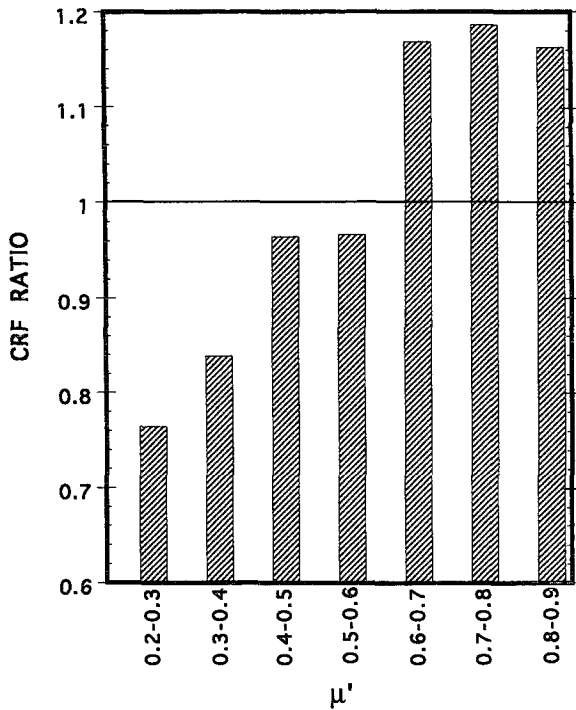


FIG. 16. Histogram of \overline{CRF}_R as a function of μ' . The trend of increasing \overline{CRF}_R with SZA as the sun approaches the horizon (smaller μ') is consistent with an increase in clear-sky absorption with μ' and an independence of cloudy-sky absorption with μ' causing \overline{CRF}_R to switch over from a value greater than 1.0 to a value less than 1.0. This observation is in agreement with Fig. 15 where it was seen that, as the zenith angle increases, the average clear-sky absorption grows until it exceeds that of cloudy sky.

view the latest reports of excessive absorption in an attempt to determine where and why they differ from other studies.

a. Cess et al. (1995)

These authors presented results for collocated satellite and surface pyranometers for five locations from Barrow, Alaska, to Cape Grim, Tasmania. Based both on an analysis by the direct method and, separately, by plots of TOA albedo versus transmission, they concluded that the data support a \overline{CRF}_R of 1.5, which is invariant with respect to location, season, cloud amount, and cloud height. They point out that this \overline{CRF}_R implies a global, cloud-induced, atmospheric absorption of 25 W m^{-2} greater than that calculated by GCMs (24-h average).

1) THE DIRECT METHOD

In Cess et al. (1995) the only dataset treated by the direct method was the BAO/GOES set from Boulder. The authors chose to use the upper-envelope method for determining clear-sky references for both TOA and

surface fluxes, a method that we have demonstrated will generally yield an unreasonably high \overline{CRF}_R . They found $\overline{CRF}_{\text{toa}} = -63.2 \text{ W m}^{-2}$ and $\overline{CRF}_c = -92.6$ (day-side values) and, hence, a \overline{CRF}_R of 1.47. Unfortunately, no uncertainties are given for any of these numbers, but these can be estimated from our current work. From Minnis et al. (1995), we have a minimum uncertainty of $\pm 7 \text{ W m}^{-2}$ due solely to the conversion from narrow- to broadband TOA fluxes. For the ARM data we estimated that the bias inherent in the upper-envelope clear-sky reference could be as much as 30 W m^{-2} . If we assume that this bias is roughly proportional to the $\overline{CRF}_{\text{toa}}$, then a bias of anywhere from 0 to 20 W m^{-2} on \overline{CRF}_c would not be unreasonable for the BAO GOES data. Combining these two uncertainties yields an absorption in excess of clear sky (for Boulder) anywhere from 3 to 37 W m^{-2} , and a \overline{CRF}_R anywhere from 1.0 to 1.7.

2) TOA ALBEDO VERSUS TRANSMISSION

The same authors also derived values for \overline{CRF}_R from all five sites from plots of TOA albedo versus transmission. We have already discussed our concerns with this method, but an additional concern with regard to how this method was implemented by Cess et al. (1995) also needs to be discussed. The authors chose to derive their slopes by regressing TOA albedo against transmission. This statistical treatment, which minimizes only deviations in TOA albedo, is inappropriate to a dataset in which both variables are subject to similar measurement uncertainties as is, we believe, the case here. (The surface detector suffers from a variable field of view that depends on cloud height, and is mostly sensitive to clouds when they happen to be on a line between it and the sun, whereas the satellite views a large area but only a small scattering angle.) Arking et al. (1995) recently presented a statistical analysis of this question and concluded that, because of the problems associated with viewing angle of the surface pyranometer, most of the uncertainty should be associated with the surface data. They recommend regressing transmission against TOA albedo, exactly the opposite of the approach taken in Cess et al. (1995).

Cess et al. (1995) offer no reason for their choice of fitting procedure; however, this choice produces \overline{CRF}_R 's that are significantly larger than justified by the data, for the following reason. Given a dataset with a small correlation coefficient R , the derived slope is quite sensitive to the fitting procedure that is used. For instance, it is a well-known statistical theorem (Rider 1939) that the magnitude of the slope derived by regressing (in this case) α_{toa} against transmission will be a factor of R^2 smaller than that of the slope obtained by regressing transmission against α_{toa} . Cess et al. (1995) do not report R values but, given the large scatter in the data they show (BAO GOES), we estimate $R = 0.9$. Then, with reference to Eq. (5), and given

their reported slope of -0.59 and average surface albedo of 0.17 , a simple reversal of the regression variables (as was suggested by Arking et al. 1995) would give a $\overline{\text{CRF}}_R$ for their data of

$$\overline{\text{CRF}}_R = \frac{(1 - 0.17)(0.9)^2}{0.59} = 1.1,$$

which agrees with both the models and the ARM IOP data.

It is also revealing to recall (see section 3c) that a BAO ERBE dataset, when analyzed by Nemesure et al. (1994) using the two variable, flux to flux method, gave a $\overline{\text{CRF}}_R$ of 0.98 ± 0.05 , which, as these investigators point out, is indicative of neutral cloud forcing. In contrast, analysis of the *very same* data by the same group (Cess et al. 1995), but using the TOA albedo slope method yielded a CRF_R of 1.59 ± 0.14 and inferred excessive absorption. Given the limitations of both methods, the fact that the two analyses produced very different results is not surprising. What is surprising, and should have suggested a more cautious interpretation, is that the error bars for the two results are not even close to overlapping. *This serious deficiency is due to the practice of considering only those uncertainties that are given formally by least squares fits of the data to postulated functional relationships. Uncertainties derived in this way are at best estimates of precision. They do not reflect the true accuracy of the inferred CRF ratio, which depends both on systematic errors, and on assumptions employed in the analyses.*

b. Pilewskie and Valero (1995)

Pilewskie and Valero (1995) presented results from measurements of mostly very thin clouds between 8 and 20 km, using two aircraft, one above and one below the clouds. They used the direct method to estimate a CRF_R of 1.68 for that section of the atmosphere. This ratio was then converted, by way of atmospheric radiation models, to a total column $\overline{\text{CRF}}_R$ of 1.5. However, a perusal of the data from their Fig. 4 indicates that $\overline{\text{CRF}}_R$ is very poorly constrained; at least for the 8–20-km fraction of the atmosphere where it varies between 0.9 and 2.4.

As in Cess et al. (1995) the authors here also used a plot of TOA albedo versus transmission. Again without justification, they chose a regression procedure that minimized deviations only in the albedo, while ignoring possible measurement uncertainties in the transmission. Considering the similarity between the two aircraft, it seems to us more reasonable to use a regression procedure that minimizes equally deviations in both variables. The effect on $\overline{\text{CRF}}_R$ of minimizing only the deviations in the albedo is here even more extreme. From their regression procedure Pilewskie and Valero calculated a $\beta = 0.5$, much smaller than that predicted by models, but seemingly in agreement

with Cess et al. (1995). Although here too, R , the coefficient of correlation, was not reported, we analyzed the published dataset and found R to be 0.76, and thus the value of β from the converse regression to be a factor of $0.76^{-2} = 1.7$ greater than that reported, now greater than that predicted by models. Clearly, “the slopes” of these noisy datasets are as much results of the choice of fitting algorithm as they are of the data themselves.

If we take the geometrically averaged slope, which amounts to treating the data from the two aircraft on an equal footing, we find an average $\overline{\text{CRF}}_R$ of 1.1, again in agreement with models and the ARM IOP data as analyzed here.

c. Ramanathan et al. (1995)

Ramanathan et al. (1995) presented results for the Western Pacific warm pool. Five years (1985–89) of ERBE satellite observations were used to generate both the average $\overline{\text{CRF}}_{\text{toa}}$ and, through the Li transfer algorithm (Li et al. 1993), the necessary clear-sky, surface reference. Instead of using pyranometers to determine the surface all-sky SW flux, they treated the top, mixed layer of the warm pool as a giant calorimeter assumed to be in a steady state. By determining all the other heat fluxes, which contributed to the steady-state temperature, they attempted to calculate the surface all-sky SW flux. To do this they estimated the net longwave cooling, evaporative cooling, horizontal advection, downward entrainment, and a few other, smaller, terms. Each of the required terms was derived on the basis of reported experimental or model results; these were obtained at various times, some of which match the period of satellite observation although most do not. The five years (1984–89) of satellite data, for example, are used in conjunction with the evaporative heat flux, taken during the 1992–93 El Niño.

The authors concluded that to balance the ocean heat fluxes the $\overline{\text{CRF}}_s$ must be -100 W m^{-2} (this and the rest of the numbers in this section are reported as 24-h averages). Combined with a $\overline{\text{CRF}}_{\text{toa}}$ of -66 W m^{-2} , this yielded a $\overline{\text{CRF}}_R$ of 1.5. In terms of cloud-induced atmospheric absorption, they assert that, on average, clouds induce 34 W m^{-2} more SW atmospheric absorption than would a continually clear sky.

In their paper, however, the authors do qualify this conclusion based on *their* estimated confidence limits. They assess the actual $\overline{\text{CRF}}_s$ to be anywhere from -135 to -80 W m^{-2} (an uncertainty of 55 W m^{-2}). They estimate a bias of less than 10 W m^{-2} on $\overline{\text{CRF}}_{\text{toa}}$ (and use 6 W m^{-2}). Propagation of *their* estimated uncertainties yields a $\overline{\text{CRF}}_R$ somewhere between 1.1 and 2.2. They indeed conclude on this basis that “*we do not know whether clouds significantly enhance or have no effect on the atmospheric solar absorption.*”

In addition to the uncertainties noted above, recent experimental results (Siegel et al. 1995) suggest that

the ocean heat balance, as formulated by Ramanathan et al. (1995), is missing a term of about 35 W m^{-2} ; this term represents the SW radiation, which penetrates *beyond* the mixed layer and is therefore lost to their calorimeter. In Ramanathan et al. (1995) it was assumed that none of the SW radiation penetrates beyond the mixed layer. Inclusion of this term shifts the surface results by 35 W m^{-2} to yield an average $\overline{\text{CRF}_s}$ of 65 W m^{-2} and an average $\overline{\text{CRF}_R}$ of 1.0, again in agreement with conventional models and the ARM IOP dataset (although the uncertainties given above still preclude any meaningful conclusion).

d. Summarizing the latest reports

Our reexamination of the latest reports of excessive cloud-induced absorption (Cess et al. 1995; Ramanathan et al. 1995; Pilewskie and Valero 1995) reveals that, once the appropriate uncertainties are considered, the results presented in all three papers span both conventional as well as unexplained, “missing” physics. Moreover, we have shown that in all three papers the chosen methods of analysis introduced substantial biases toward higher $\overline{\text{CRF}_R}$. On this basis we conclude that these studies do not provide compelling reasons to question our basic understanding of the interactions of clouds with SW radiation.

6. Conclusions

a. Methods of analysis

We have presented a comparative study of the various methods that have been used to analyze collocated surface and satellite radiation measurements for the purpose of determining cloud radiative impact. Each method was applied to the ARM IOP dataset in order to examine its strengths and limitations. The methods we find most useful are those described in section 3D, that of the CRF_s versus CRF_{toa} slope and its normalized analog. These methods are reasonably independent of the usual errors in the choice of clear-sky reference and can be used for hourly, daily, or monthly averaged data as was demonstrated by Li et al. (1996). The influence of SZA is greatly reduced by examining forcing rather than fluxes. The assumption of linearity in the dependence of CRF_s on CRF_{toa} , at least for the present dataset, is reasonably fulfilled.

In general, it is clear that one’s conclusions concerning cloud-induced absorption can depend to a large degree on small, unrecognized flaws in the methods and/or inconsistencies between the assumptions necessary to a given method and those supportable by the data. Further, we point out that, even if a perfect method was available, the whole notion of cloud-induced absorption (in excess of clear-sky absorption) has meaning only when “clear sky” has been explicitly defined; small differences among clear-sky references can yield

remarkably different “excess absorptions.” In this context, any useful comparisons of field data with models additionally require that the experimental and modeled clear skies be demonstrably similar.

b. ARM IOP data

A summation of atmospheric properties observed during the ARM IOP of April 1994 is given in the cartoon in the upper panel of Fig. 17; for comparison, the lower panel reproduces a similar figure from Kerr (1995) that summarizes the findings from three articles in *Science* (Cess et al. 1995; Ramanathan et al. 1995; Pilewskie and Valero 1995), which report excessive absorption. We realize that the latter figure (as is ours)

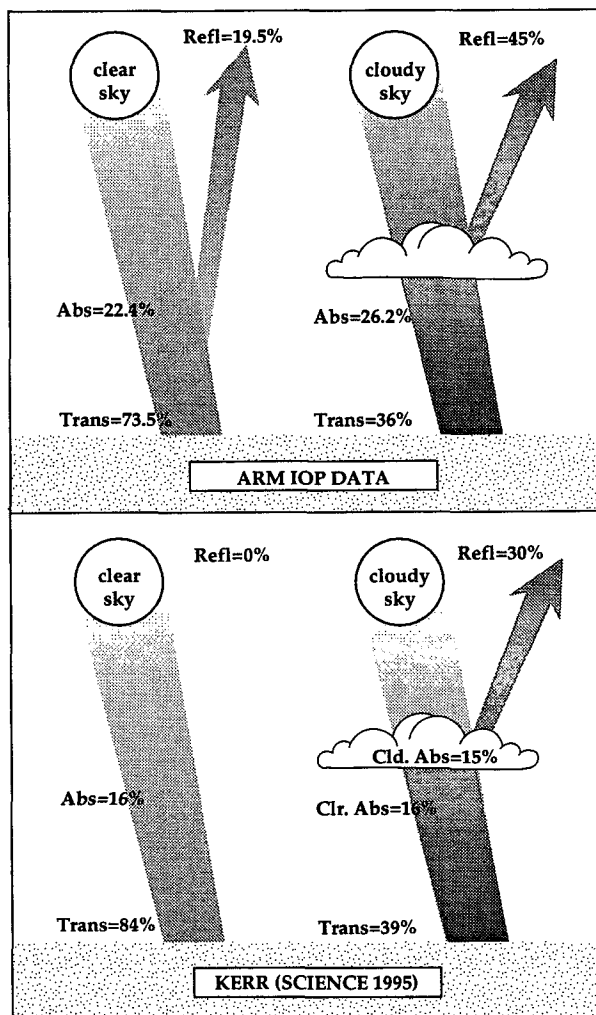


FIG. 17. This figure contrasts the findings of the present study with those presented by Kerr (1995). Earth’s atmosphere, as observed in Oklahoma during the ARM IOP, is presented in the top panel, while the bottom panel represents the atmosphere as summarized by Kerr on the basis of three recent articles in *Science*. The two differ in their depictions of both clear and cloudy skies (see text for explanation).

is schematic in nature, but we also note that the numbers in this figure were carefully chosen to reproduce the reported $\overline{\text{CRF}_R}$ of 1.5, the average $\overline{\text{CRF}_{\text{toa}}}$ of -50 W m^{-2} , and the average cloud-induced excess absorption of 25 W m^{-2} . It is in this context that we feel a comparison between the two depicted atmospheres may provide some insight as to where the differences lie.

We find the dissimilarity between the earth's atmosphere as we infer it from the Oklahoma data and as it is presented in Kerr (1995) to be vast. Remarkably, the differences between the two clear skies are as large as those pertaining to the cloudy skies. According to the present Oklahoma data, as well as Liou (1992), Laszlo and Pinker (1993), and Arking et al. (1995), the average clear-sky absorption is 22%, in contrast with only 16% clear-sky absorption for Kerr's atmosphere. Similarly, the clear-sky transmissions differ by about 10%. Clouds at the ARM site increase atmospheric column absorption by 4%, which is consistent with the "traditional" view of clouds (Kerr 1995; Liou 1992). Again, the average of 4% increased SW absorption refers to the entire column and does not imply that clouds absorb only 4%. In actuality, clouds absorb, on the average, much more, but by reflecting much of the light back to space they tend to decrease the absorption below them such that the net effect on SW absorption is only 4%. A very different picture of the alteration of atmospheric absorption by clouds is presented in Kerr (1995). To produce a $\overline{\text{CRF}_R}$ of 1.5, Kerr's clouds absorb an additional 15% *without decreasing the absorption by the clear portion of the atmosphere* despite the loss of 45% of the SW radiation due to cloud-induced reflection and absorption. Such an atmosphere must imply that the mere presence of clouds alters the properties of the *clear air* as to almost double its SW absorptivity.

We have also investigated the sensitivities of cloud-induced atmospheric absorption and $\overline{\text{CRF}_R}$ to changing atmospheric conditions. We find that both are strongly affected by cloud amounts and SZA (and, by extension, latitude, and season). We expect that a strong dependence on cloud altitude is also present, as shown by Li and Moreau 1996. Due to these large and systematic variations, we question the usefulness of the concept of $\overline{\text{CRF}_R}$.

c. Anomalous absorption

The results of our analysis of the ARM IOP surface data, in conjunction with the GOES observations, are consistent with the possibility of a *small* cloud-induced increase of atmospheric column absorption as reported in various studies reviewed by Stephens and Tsay (1990) and also in those more recently reported by Li et al. (1995), Li and Moreau 1996, Hayasaka et al. (1995), Laszlo and Pinker (1993), and Arking et al. (1995). All these studies indicate that clouds may induce an increase in SW atmospheric absorption, which

is in *slight* excess over those of clear sky. At the same time our results exclude the possibility of an absorption of the magnitude reported in Cess et al. (1995), Ramanathan et al. (1995), and Pilewskie and Valero (1995). All of these three papers can be reconciled with the present results if account is taken either of the true uncertainties in their reported numbers or of the uniform biases inherent in their methods of analysis.

We are still concerned about biases that may result when the visible radiances measured by GOES are used to infer total shortwave fluxes. To address this concern we intend to carry out a similar investigation with five years of surface data from Samoa in conjunction with ERBS observations of TOA radiances.

Acknowledgments. The conversion of data from net CDF to ascii, extraction of subsets of data, averaging of the data, and the calculations of solar zenith angle were performed by L. Benedict, A. Cialella, and T. Kwan of the Scientific Information Systems Group at BNL directed by J. Tichler. We thank A. Arking, L. Newman, P. Falkowski, and S. Schwartz for useful discussions.

This research was performed as part of the Unmanned Aerospace Vehicle Program under sponsorship of the U.S. Department of Energy, Contract DE-AC02-76CH00016.

APPENDIX

Derivation of Eq. (5)

a. Definition of terms

Superscripts of *a* and *clr* denote all-sky data and clear-sky reference, respectively. Subscripts of *toa* and *s* denote top of the atmosphere and surface, respectively.

Here, *I* is insolation, *T* transmission, α albedo, $\beta = -d\alpha_{\text{toa}}/dT$, *F* net flux, $F_{\text{toa}} = (1 - \alpha_{\text{toa}})I_{\text{toa}}$, $F_s = (1 - \alpha_s)I_s$, \bar{X} denotes the mean value of *X*, and $\bar{\bar{X}}$ denotes a power-weighted average such as

$$\bar{\alpha}_{\text{toa}} = 1 - \frac{\overline{F_{\text{toa}}}}{\overline{I_{\text{toa}}}}$$

and

$$\bar{\bar{T}} = \frac{\overline{I_s}}{\overline{I_{\text{toa}}}}$$

b. Derivation

We define for each data point: $\text{CRF}_{\text{toa}} = {}^a F_{\text{toa}} - {}^{\text{clr}} F_{\text{toa}}$, the instantaneous cloud radiative forcing at TOA referenced to a chosen "clear sky" with the identical TOA insolation. The mean TOA cloud radiative forcing is then given by

$$\overline{\text{CRF}_{\text{toa}}} = (1 - \overline{\alpha_{\text{toa}}}) \overline{I_{\text{toa}}} - (1 - \overline{\alpha_{\text{toa}}}) \overline{I_{\text{toa}}}.$$

This average is over all conditions of cloudiness and all SZA, each all-sky point being paired with its corresponding clear-sky reference. We similarly define: $CRF_s = {}^a F_s - {}^{clr} F_s$, and again,

$$\overline{CRF_s} = (1 - \overline{{}^a \alpha_s}) \overline{{}^a I_s} - (1 - \overline{{}^{clr} \alpha_s}) \overline{{}^{clr} I_s},$$

where $\overline{{}^{clr} \alpha_s}$ is the surface albedo under typical conditions of clear sky. The CRF ratio is then

$$\frac{\overline{CRF_s}}{\overline{CRF_{toa}}} = \frac{(1 - \overline{{}^a \alpha_s}) \overline{{}^a I_s} - (1 - \overline{{}^{clr} \alpha_s}) \overline{{}^{clr} I_s}}{(1 - \overline{{}^a \alpha_{toa}}) \overline{{}^a I_{toa}} - (1 - \overline{{}^{clr} \alpha_{toa}}) \overline{{}^{clr} I_{toa}}}.$$

Since for each data point we use a clear-sky reference with an identical TOA insolation, $\overline{{}^{clr} I_{toa}} = \overline{{}^a I_{toa}} = \overline{I_{toa}}$, and

$$\frac{\overline{CRF_s}}{\overline{CRF_{toa}}} = \frac{(1 - \overline{{}^a \alpha_s}) \overline{{}^a I_s} - (1 - \overline{{}^{clr} \alpha_s}) \overline{{}^{clr} I_s}}{-\overline{I_{toa}} (\overline{{}^a \alpha_{toa}} - \overline{{}^{clr} \alpha_{toa}})}. \quad (A1)$$

To proceed with the derivation we must assume that the average surface albedo is independent of cloud cover; that is, $\overline{{}^a \alpha_s} = \overline{{}^{clr} \alpha_s} = \overline{\alpha_s}$. For the ARM site data, at least, this is a good approximation since $\overline{{}^a \alpha_s} = 0.204 \pm 0.005$ and $\overline{{}^{clr} \alpha_s} = 0.205 \pm 0.005$. Equation (A1) for the CRF ratio can now be written as

$$\frac{\overline{CRF_s}}{\overline{CRF_{toa}}} = \frac{(\overline{{}^a I_s} - \overline{{}^{clr} I_s})(1 - \overline{\alpha_s})}{-\overline{I_{toa}} (\overline{{}^a \alpha_{toa}} - \overline{{}^{clr} \alpha_{toa}})}. \quad (A2)$$

To relate the CRF ratio to the ‘‘slope’’ of a plot of TOA albedo versus transmission we need to assume that α_{toa} for all-sky is related to T as

$$\overline{{}^a \alpha_{toa}} = C_0 - \beta {}^a T, \quad (A3)$$

then

$$\begin{aligned} 1 - \frac{{}^a F_{toa}}{I_{toa}} &= C_0 - \beta \frac{{}^a I_s}{I_{toa}} \\ I_{toa} - {}^a F_{toa} &= C_0 I_{toa} - \beta {}^a I_s \\ \overline{I_{toa}} - \overline{{}^a F_{toa}} &= C_0 \overline{I_{toa}} - \beta \overline{{}^a I_s} \\ \overline{{}^a \alpha_{toa}} &= C_0 - \beta \frac{\overline{{}^a I_s}}{\overline{I_{toa}}}. \end{aligned}$$

Now we reference these quantities to clear sky by assuming that the clear-sky points lie on the same line as the all-sky points, defined by the same C_0 and β , so that we have also

$$\overline{{}^{clr} \alpha_{toa}} = C_0 - \beta \frac{\overline{{}^{clr} I_s}}{\overline{I_{toa}}}.$$

We can use the last two equations above to solve for β

$$\beta = \frac{-\overline{I_{toa}} (\overline{{}^a \alpha_{toa}} - \overline{{}^{clr} \alpha_{toa}})}{(\overline{{}^a I_s} - \overline{{}^{clr} I_s})},$$

and with (A2) we have

$$\frac{\overline{CRF_s}}{\overline{CRF_{toa}}} = \frac{(1 - \overline{\alpha_s})}{\beta}. \quad (A4)$$

Equation (A4) is the connection between the CRF ratio and β as used in several recent papers.

Whether Eq. (A4) is valid depends on how well the data support the assumptions essential to its derivation. As demonstrated in Fig. 6, the ARM IOP data clearly do not support the assumption of linearity [Eq. (A3)], moreover the very same curvature is apparent in all other datasets we have examined thus far.

The assumption that the clear-sky points lie on the same line as the all-sky data is implicit in the original assumption of linearity, since the (experimental) clear-sky points are a subset of the all-sky data. We have chosen to emphasize this point because at first glance it might seem that all the clear-sky points should cluster about a single α_{toa} , and T . But as shown in Fig. 5, variations in SZA cause even the clear-sky points to span a large range of transmission and TOA albedo, and their pattern describes a line that can be readily distinguished from the balance of the data.

The requirement that the line describing clear sky be the same as that for all sky leads to two possibilities. If the assumption is good, then β , and hence the CRF ratio, can be determined from clear-sky data alone; clearly this is senseless. On the other hand, if the assumption is incorrect, as we find for the present dataset, then Eq. (A4) is invalid and cannot be relied upon to give the correct CRF ratio.

REFERENCES

- Arking, A., M.-D. Chou, and W. L. Ridgway, 1995: On estimating the effects of clouds on atmospheric absorption based on flux observations above and below cloud level. *Geophys. Res. Lett.*, **22**, 1885–1888.
- Cess, R. D., S. Nemesure, E. G. Dutton, J. J. DeLuise, G. L. Potter, and J.-J. Morcrette, 1993: The impact of clouds on the shortwave radiation budget of the surface–atmosphere system: Interfacing measurements and models. *J. Climate*, **6**, 308–316.
- , and Coauthors, 1995: Absorption of solar radiation by clouds: Observations versus models. *Science*, **267**, 496–499.
- Chou, M.-D., A. Arking, J. Otterman, and W. L. Ridgway, 1995: The effect of clouds on atmospheric absorption of solar radiation. *Geophys. Res. Lett.*, **22**, 1885–1888.
- Foot, J. S., 1988: Some observations of the optical properties of clouds. Part I: Stratocumulus. *Quart. J. Roy. Meteor. Soc.*, **114**, 129–144.
- Hayasaka, T., N. Kikuchi, and M. Tanaka, 1995: Absorption of solar radiation by stratocumulus clouds: Aircraft measurements and theoretical calculations. *J. Appl. Meteor.*, **34**, 1047–1055.
- Herman, G. F., 1977: Solar radiation in summertime Arctic stratus clouds. *J. Atmos. Sci.*, **34**, 1423–1432.
- Kerr, R. A., 1995: Darker clouds promise brighter future for climate models. *Science*, **267**, 454.
- Laszlo, I., and R. T. Pinker, 1993: Shortwave cloud-radiative forcing at the top of the atmosphere at the surface and of the atmospheric column as determined from ISCCP C1 data. *J. Geophys. Res.*, **98D**, 2703–2713.
- Li, Z., H. G. Leighton, K. Masuda, and T. Takashima, 1993: Estimation of SW flux absorbed at the surface from TOA reflected flux. *J. Climate*, **6**, 317–330.

- , H. W. Barker, and L. Moreau, 1995: The variable effect of clouds on atmospheric absorption of solar radiation. *Nature*, **376**, 486–490.
- , and L. Moreau, 1996: Alteration of atmospheric solar absorption by clouds: Simulation and observation. *J. Appl. Meteor.*, **35**, 653–670.
- Liou, K-N, 1992: *Radiation and Cloud Processes in the Atmosphere. Theory, Observation, and Modeling*. Oxford University Press, 487 pp.
- Minnis, P., W. L. Smith Jr., D. P. Garber, J. K. Ayers, and D. R. Doelling, 1995: Cloud properties derived from GOES-7 for spring 1994 ARM intensive observing period using version 1.0.0. of ARM satellite data analysis program. NASA reference publication 1366. [Available on-line from <http://tech-reports.larc.nasa.gov/ltrs/ltrs.html>]
- Nakajima, T., M. D. King, J. D. Spinhirne, and L. F. Radke, 1991: Determination of the optical thickness and effective particle radius of clouds from reflected solar radiation measurements. Part II: Marine stratocumulus observations. *J. Atmos. Sci.*, **48**, 728–750.
- Nemesure, S., R. D. Cess, E. G. Dutton, J. J. DeLuisi, Z. Li, and H. G. Leighton, 1994: Impact of clouds on the shortwave radiation budget of the surface-atmosphere system for snow-covered surfaces. *J. Climate*, **7**, 579–585.
- Pilewskie, P., and F. P. J. Valero, 1995: Direct observations of excess solar absorption by clouds. *Science*, **257**, 1626–1629.
- Ramanathan, V., B. Subasilar, G. J. Zhang, W. Conant, R. D. Cess, J. T. Kiehl, H. Grassl, and L. Shi, 1995: Warm pool heat budget and shortwave cloud forcing: A missing physics? *Science*, **267**, 499–503.
- Rawlins, F., 1989: Aircraft measurements of the solar absorption by broken cloud fields: A case study. *Quart. J. Roy. Meteor. Soc.*, **115**, 365–382.
- Reynolds, D. W., T. H. Vonder Haar, and S. K. Cox, 1975: The effect of solar radiation absorption in the tropical troposphere. *J. Appl. Meteor.*, **14**, 433–444.
- Rider, P. R., 1939: *An Introduction to Modern Statistical Methods*. Wiley and Sons, 345 pp.
- Robinson, G. D., 1959: Some observations from aircraft of surface albedo and the albedo and absorption of cloud. *Arch. Meteor. Geophys. Bioklimatol.*, **B9**, 28–41.
- Siegel, D. A., J. C. Ohlmann, L. Washburn, R. R. Bidigare, C. T. Nosse, E. Fields, and Y. Zhou, 1995: Solar radiation, phytoplankton pigments and the radiant heating of the equatorial pacific warm pool. *J. Geophys. Res.*, **100C**, 4885–4891.
- Slingo, A., and H. M. Schrecker, 1982: On the shortwave radiative properties of stratiform water clouds. *Quart. J. Roy. Meteor. Soc.*, **108**, 407–426.
- Stephens, G. L., 1996: How much solar radiation do clouds absorb? *Science*, **271**, 1131–1133.
- , and C. M. R. Platt, 1987: Aircraft observations of the radiative and microphysical properties of stratocumulus and cumulus cloud fields. *J. Climate Appl. Meteor.*, **26**, 1243–1269.
- , and S-C. Tsay, 1990: On the cloud absorption anomaly. *Quart. J. Roy. Meteor. Soc.*, **116**, 671–704.
- Wiscombe, W. J., 1995: An absorbing mystery. *Nature*, **376**, 466–467.